

The role of iodine in plant defence against *Botrytis cinerea*

Sara Beltrami^{a,c}, Lorenzo Di Paco^a, Claudia Pisuttu^b, Lorenzo Mariotti^b,
Alessandra Marchica^{a,b}, Elisa Pellegrini^b, Sabrina Sarrocco^b, Cristina Nali^b,
Pierdomenico Perata^a, Claudia Kiferle^{a,*}

^a PlantLab, Institute of Plant Sciences, Sant'Anna School of Advanced Studies, Pisa, Italy

^b Department of Agriculture, Food and Environment, University of Pisa, Italy

^c Department of Agriculture, Food, Environment and Forestry (DAGRI), University of Florence, Italy

ARTICLE INFO

Keywords:

Arabidopsis thaliana

Botrytis cinerea

Defence signalling

Iodine

Plant nutrition

Transcriptomics

ABSTRACT

Iodine has been recently defined as a plant nutrient, triggering beneficial outcomes in terms of plant fitness and crop quality. In the present study, we demonstrated that iodine boosts *Arabidopsis* tolerance against the necrotrophic fungal pathogen *Botrytis cinerea*. At micromolar concentrations, we found that iodine activated a broad spectrum of immune-like responses, stimulating the transient accumulation of H₂O₂, likely acting as a second messenger. Iodine activated three major hormonal players involved in plant defence, namely, salicylic acid, jasmonic acid and ethylene. Several pathogenesis-related (PR) genes, particularly PR2 and PR5, were also strongly induced by iodine. The use of *Arabidopsis* mutants impaired in SA, JA or ET biosynthesis/signalling allowed us to demonstrate the central role of JA in the iodine-induced resistance to *B. cinerea*. Nevertheless, the wide range of defence-like responses triggered by iodine suggests its potential effectiveness against a broad spectrum of biotic agents. Integrating iodine in plant nutritional programs thus represents a promising, eco-friendly, and easy-to-apply tool to fight against pathogen attacks, which could be alternative/additional to using traditional pesticides.

Abbreviations

ET	ethylene,
JA	jasmonic acid,
PBI	post <i>B. cinerea</i> infection,
PIT	post iodine treatment,
PR	pathogenesis-related,
SA	salicylic acid.

1. Introduction

Iodine has been recently classified as a plant nutrient (Brown et al., 2022). In fact, the addition of micromolar amounts of iodized salts to nutrient culture solutions promotes plant growth and productivity, flowering time, and abiotic stress resilience. In addition, iodinated proteins have been identified in shoot and root tissues of *Arabidopsis thaliana*, possibly affecting the functionality of several physiological

processes in which they are involved (Kiferle et al., 2021; Riyazuddin et al., 2023).

At a transcriptional level, applying iodine in the micromolar range regulates the expression of several genes involved in the plant response to abiotic and biotic stresses (Kiferle et al., 2021; Smoleń et al., 2023). A clear correlation between several iodine-responsive genes and those typically modulated in the presence of fungal infection, salicylic acid (SA) or synthetic analogues of SA, has been demonstrated (Kiferle et al., 2021).

Biochemical determinations support the link between iodine and the SA pathway, as the addition of micromolar amounts of potassium iodide (KI) or potassium iodate (KIO₃) in nutrient solution increased the SA content in fruits and roots of iodine-treated tomato plants (Halka et al., 2019) as well as in the root secretions of lettuce plants (Smoleń et al., 2021).

Salicylic acid is a phytohormone involved in a plethora of mechanisms related to plant growth, metabolism, and development and is also

* Corresponding author at: PlantLab, Center of Plant Sciences, Scuola Superiore Sant'Anna, Piazza Martiri della Libertà, 33, 56127, Pisa, Italy.

E-mail addresses: sara.beltrami@unifi.it (S. Beltrami), Lorenzo.DiPaco@santannapisa.it (L. Di Paco), claudia.pisuttu@agr.unipi.it (C. Pisuttu), lorenzo.mariotti@unipi.it (L. Mariotti), Alessandra.Marchica@santannapisa.it (A. Marchica), elisa.pellegrini@unipi.it (E. Pellegrini), sabrina.sarrocco@unipi.it (S. Sarrocco), cristina.nali@unipi.it (C. Nali), Pierdomenico.Perata@santannapisa.it (P. Perata), Claudia.Kiferle@santannapisa.it (C. Kiferle).

<https://doi.org/10.1016/j.stress.2024.100723>

Received 12 September 2024; Received in revised form 6 December 2024; Accepted 21 December 2024

Available online 29 December 2024

2667-064X/© 2025 The Authors. Published by Elsevier B.V. This is an open access article under the CC BY license (<http://creativecommons.org/licenses/by/4.0/>).

considered a key signal molecule involved in abiotic and biotic stress responses (Dempsey et al., 2011). The protective effect of very low amounts of iodine against adverse environmental conditions, such as salinity or heavy metals, is well documented in systematic reviews (e.g., Zhang et al., 2023). In contrast, to the best of our knowledge, the possibility of exploiting iodine, applied at very low concentrations, as a modulator of plant defence responses has never been investigated.

The correct management of mineral nutrients is crucial for plant protection (Tripathi et al., 2022) and represents a sustainable tool to limit the use of pesticides, which constitute the most common and effective agricultural practice adopted to limit crop diseases (Zubrod et al., 2019). The high economic cost and the impact of synthetic products on human health, the environment and food quality (“food safety”) have raised great concern by increasing the demand for alternative and more sustainable strategies that are able to ensure crop protection.

The aim of the present study was to evaluate the protective effect of iodine-integrated plant nutrition on *Arabidopsis* plants infected with *Botrytis cinerea*, which is a model for the study of necrotrophic fungal pathogens and is responsible for massive reductions in agricultural production worldwide (Cheung et al., 2020).

In order to characterize the mechanisms of iodine-enhanced plant defence, we performed an extensive array of biochemical and molecular analyses on both the shoot and root tissues of iodine-treated plants prior to *B. cinerea* inoculation and after fungal exposure. In detail, we evaluated the endogenous levels of SA and the other two major phytohormones involved in biotic stress tolerance mechanisms, namely, jasmonic acid (JA) and ethylene (ET) (Ding et al., 2022; Vlot et al., 2021). We also quantified the tissue content of hydrogen peroxide (H_2O_2), which is considered a signalling molecule that regulates a multitude of physiological processes, including host-pathogen recognition/resistance mechanisms (Saxena et al., 2016; Smirnov and Arnaud, 2019).

Finally, we characterized the transcriptional response of genes related to SA, JA and ET biosynthesis and signalling, and that of pathogenesis-related (PR) genes, which are strictly involved in plant defence (Ali et al., 2018; Dos Santos and Luiz Franco, 2023).

2. Materials and methods

2.1. Plant material and cultivation system

Arabidopsis thaliana ecotype Columbia 0 (Col-0) was used throughout the study. Other genotypes used were *sid2-3* (N542603, which is defective in SA biosynthesis; Pluharová et al., 2019), *jar1-1* (N8072, which is impaired in jasmonyl-L-isoleucine (Ja-Ile) biosynthesis, the active form of JA; Staswick et al., 1992) and *acs2-1acs6-1* (N8072, which is defective in ET biosynthesis; Tsuchisaka et al., 2009). All the mutant lines were purchased from the Nottingham Arabidopsis Stock Centre (NASC, Nottingham, UK) and were in the Col-0 background. The segregating lines (*sid2-3* and *acs2-1acs6-1*) were checked for homozygosity via PCR (Supplementary Table S1).

Arabidopsis seeds were sown on rockwool plugs and stratified at 4 °C in the dark for 48 h. Germinating seeds were then moved to a growth chamber set as follows: 22 °C day/18 °C night with a 12 h photoperiod, a quantum irradiance of 100 $\mu\text{mol photons m}^{-2}\text{s}^{-1}$ and a relative humidity close to 35 %. The plants were grown on a floating hydroponic system using a base nutrient solution, which was prepared by dissolving ultrapure laboratory salts in double-distilled water: 1.25 mM KNO_3 , 1.50 mM $Ca(NO_3)_2$, 0.75 mM $MgSO_4$, 0.50 mM KH_2PO_4 , 50 μM KCl, 50 μM H_3BO_3 , 10 μM $MnSO_4$, 2.0 μM $ZnSO_4$, 1.5 μM $CuSO_4$, 0.075 μM $(NH_4)_6Mo_7O_{24}$ and 72 μM Fe-EDTA. During the preparation, the electrical conductivity (EC) and pH of the nutrient solution ranged between 0.5–0.6 dS m^{-1} and 5.7–6.0 (adjusted with diluted H_2SO_4), respectively. The hydroponic trays were covered with black plastic film to avoid light on the nutrient solution and thus algae formation. The iodine concentration in the solution was below the detection limit (8 nM), as

determined by ICP-MS analysis.

Arabidopsis plants that were homogeneous in size and number of leaves were selected and cultured in an iodine-free solution for four weeks. The plants were then treated with different concentrations of KI (0, 10 and 30 μM) via the addition of salt to the basal nutrient solution. The iodine treatments used in the SA, JA- and ET-mutant experiments were limited to 0 and 30 μM KI.

The plants were distributed in two hydroponic trays/treatment, and a total of 30 plants were cultivated for each experimental condition (15 plants/tray). The nutrient solutions were replaced twice a week to maintain their nutritional composition, limiting the pH and EC fluctuations as much as possible.

During the growing cycle, a group of plants was subjected to molecular and biochemical analyses to evaluate the effect of iodine in the absence of the pathogen (pre-infection characterization), whereas a subset of plants subjected to a 72 h KI pre-treatment was inoculated with *B. cinerea* and subsequently characterized (post-infection characterization). In the latter case, KI was generally maintained in the nutrient solution until the end of the trial, except for a single experiment, where plants were removed from the KI-containing solution immediately after pathogen inoculation. Plants were sampled at different time points depending on the specific goal of each experiment, as fully described in the devoted sections and summarized in Supplementary Fig. S1.

Unless otherwise specified, all the analytical determinations performed and described below were conducted on the Col-0 genotype.

2.2. Plant inoculation with *Botrytis cinerea*

The *B. cinerea* strains used in the present work, as well as the methods followed for pathogen cultivation and inoculum preparation, are those reported by Valeri et al. (2021). *Arabidopsis* plants were inoculated with *B. cinerea* three days post iodine treatment (PIT). Plant inoculation was conducted by placing 5 μl of a spore suspension (1×10^6 conidia ml^{-1}) on the leaf surface (hereafter, 1 drop). The number of inoculated leaves/plant as well as that of drops/leaves varied depending on the specific experimental goals, as specified in the subsections below for each experiment. In all the cases, one group of plants, pre-treated or not pre-treated with KI, whose leaves were infiltrated only with the buffer alone (mock), was used as a negative control. After inoculation, the plants were placed in plastic boxes enclosed with cling film in the presence of a steam source (to maintain high humidity) and cultured in a biological incubator (Percival Scientific, Perry, IA, USA) under the same environmental conditions previously reported for the growth chamber.

2.3. Symptom evaluation

The progression of fungal infection was monitored by characterizing the pathogenic lesions that originated over time after *B. cinerea* inoculation.

All the rosette leaves were inoculated (1 drop/leaf), and three days post *B. cinerea* infection (PBI), a quantitative analysis of lesions was performed on Col-0 plants by scanning infected leaves and measuring the lesion area using ImageJ v1.53k (<https://imagej.nih.gov/ij/>). The percentage of symptomatic leaves was also calculated by counting the number of diseased leaves and reporting it to the total number of inoculated ones. A qualitative image-based evaluation of the symptoms was performed on Col-0 and SA-, JA- and ET- mutants at five days PBI by scoring the lesion types according to the following scale: 1, no infection; 2, light browning corresponding to the inoculum droplet; 3, strong browning in the local lesion/yellow leaf; and 4, dark brown/necrotic leaf. The percentage of leaves belonging to the different classes was then calculated. Determinations (quantitative and qualitative analyses performed at 3 and 5 days of PBI, respectively) were performed by sampling and characterizing all the leaves from 15 plants.

To evaluate the residual effect of iodine on fungal growth, leaf symptoms were also characterized in plants (Col-0), which, once

inoculated, were transferred to an iodine-free nutrient solution, which was used until the end of the trial. In this case, five fully expanded and equally aged leaves were inoculated (1 drop/leaf), and the lesions were visually scored at five days PBI, as previously described.

2.4. Fungal growth

The effect of iodine on fungal growth was daily characterized via microscopy (Leica MZ FLUI stereomicroscope equipped with a Leica DC 300F digital camera). Leaves (Col-0) were analysed starting from *B. cinerea* inoculation until the onset of fungal sporulation. Six biological replicates, each consisting of a single leaf, were observed at each time point for all the KI treatments.

2.5. In vitro effect of iodine on *Botrytis cinerea* mycelial growth

Agar plugs (ϕ 0.5 cm) made from actively growing colonies of *B. cinerea* were transferred to potato dextrose agar (PDA) plates enriched with four different KI concentrations (0, 10, 30 and 100 μM – 10 plates/treatment). To avoid contamination, the KI solutions were filtered (MF-Millipore™ membrane filter; 0.22 μm pore size) before being added to the growing media. Dishes were randomly distributed in an incubator under the same growing conditions used for pathogen propagation (Valeri et al. 2021). The fungal radial growth was measured daily until colonies reached the edge of the plates, and the morphology of the fungus was visually monitored within the same timeframe.

2.6. Quantification of salicylic acid and jasmonic acid contents

The SA and JA contents were determined in Col-0 plants collected at 3 days PIT or 5 days PBI (1 drop/leaf). In the latter case, determinations were also performed on mock-treated plants.

Analytical determinations were performed on root and leaf samples, which were immediately frozen in liquid nitrogen at collection and stored at $-80\text{ }^{\circ}\text{C}$ until further analysis.

The conjugated and free SA contents were determined according to Pellegrini et al. (2013), with some modifications. Frozen samples (100 mg) were added to 1 ml 90 % (v/v) methanol, vortexed and sonicated for 10 min. After centrifugation at 10,000 g for 15 min at room temperature, the supernatant was transferred, and the pellet was re-extracted in 0.5 ml 100 % (v/v) methanol following the same procedure. The supernatants from both extractions were combined and evaporated under vacuum at $35\text{ }^{\circ}\text{C}$ (RVC 2–25 CDplus, Martin Christ Gefriertrocknungsanlagen GmbH, Germany). The residue was resuspended in 0.25 ml of 5 % (w/v) trichloroacetic acid (TCA) and partitioned twice into 0.8 ml of a 1:1 (v/v) mixture of ethyl acetate/cyclohexane. The upper phase containing free SA was concentrated at $35\text{ }^{\circ}\text{C}$ under vacuum, and the lower aqueous phase (with conjugated SA) was hydrolysed by adding 0.3 ml of 8 N HCl and incubating for 60 min at $80\text{ }^{\circ}\text{C}$. Salicylic acid collected from the upper phase and recovered from the lower phase was combined and dissolved in 600 μl of the mobile phase, which contained 0.2 M sodium acetate buffer (pH 5.5), water (90 %) and methanol (10 %). The separation was performed at $40\text{ }^{\circ}\text{C}$ by an ultra-high pressure liquid chromatography (UHPLC) Dionex UltiMate 3000 system equipped with an Acclaim 120 C18 column (5 μm particle size, 4.6 mm internal diameter x 150 mm length) and an UltiMate™ 3000 fluorescence detector (Thermo Scientific, Wallyham, MA, USA) with excitation at 305 nm and emission at 407 nm. The flow rate was 0.8 ml min^{-1} . To quantify the SA content, known amounts of pure standard (0.1–25 $\mu\text{g ml}^{-1}$) were injected into the UHPLC system, and an equation correlating the peak area to the SA concentration was formulated (Supplementary Figure S2). The quantifications reported in the present paper refer to the total SA (sum of free and conjugated SA).

Jasmonic acid was determined via GC–MS according to Huang et al. (2015), with minor modifications. Frozen samples (100 mg fresh weight,

FW) were added to 1 mL of 80 % methanol, sonicated for 10 min, vortexed for 1 h and centrifuged at 13,000 g for 30 min at $4\text{ }^{\circ}\text{C}$. The supernatants were filtered and evaporated at $35\text{ }^{\circ}\text{C}$ under vacuum, and the residue was resuspended in ethyl acetate. The extract was injected into a GC–MS (Agilent 8890B gas chromatograph, equipped with an Agilent 5977B single quadrupole mass detector and an Agilent DB-5MS (UI) capillary column (30 m x 0.25 mm; coating thickness 0.25 μm ; Agilent Technologies Inc., Santa Clara, CA, USA). The analytical conditions were as follows: the carrier gas was helium with a flow rate of 1 ml min^{-1} , and the injector and the transfer line were set at $250\text{ }^{\circ}\text{C}$. The temperature program was as follows: the initial column temperature was set at $70\text{ }^{\circ}\text{C}$ for 4 min, which was increased to $300\text{ }^{\circ}\text{C}$ at $10\text{ }^{\circ}\text{C min}^{-1}$. The source and quadrupole temperatures were set at 230 and $150\text{ }^{\circ}\text{C}$, respectively. The mass data were collected in the electron impact mode at 70 eV with a scan range of 40–500 m/z, and the quantification was performed in the selected-ion monitoring mode at m/z 210 amu by comparison with the reference standard using a MassHunter Workstation (version 10.0, Agilent Technologies Inc.).

The endogenous levels of SA and JA were expressed as $\mu\text{g g}^{-1}$ FW, representing the mean of three replicates, each consisting of a pool of samples derived from five different plants.

2.7. Quantification of ethylene production

Three different experiments were performed to measure the effects of iodine and *B. cinerea* treatments, alone or in combination, on Arabidopsis (Col-0) ET production.

First, a pre-infection experiment was performed to quantify ET production due to iodine treatments (0, 10 and 30 μM KI). Determinations were performed at T-0 (immediately prior to *B. cinerea* inoculation) and at 0.5, 1, 2, 4, 8, 12, 24, 48 and 72 h. A second experiment was run to identify the peak of ET emission due to *B. cinerea* infection by measuring the gaseous emissions of mock and inoculated plants in the absence of iodine. In this experiment, all the leaves were inoculated (1 drop/leaf), and ET emission was quantified at T-0 and after 0.5, 1, 2, 3, 4, 8, 12, 24 and 48 h PBI. In the third experiment, the combined effect of iodine and *B. cinerea* was studied. ET emission was measured at 1, 2 and 3 h following pathogen inoculation, which was performed on all leaves (1 drop/leaf – Col-0) of previously iodine-treated plants (72 h PIT - 0, 10 or 30 μM KI; a group of mock plants was inserted).

In all the experiments, ET production was measured by enclosing a single plant (isolated by gently removing the rockwool plug from the cultivation system, being careful not to damage the root system) in an air-tight glass container (15 ml). Gas samples (1 ml) were taken from the headspace of containers (through a hypodermic syringe) and analysed after 2 h of incubation at room temperature. The ET concentration in each sample was measured via GC–MS (as previously reported) with an Agilent HP–PLOT/Q–PT capillary column (30 m x 0.32 mm; coating thickness, 20 μm ; Agilent Technologies Inc., Santa Clara, CA, USA). The analytical conditions were as follows: the oven temperature of the GC was set to $36\text{ }^{\circ}\text{C}$, the injector temperature was $170\text{ }^{\circ}\text{C}$, the transfer line temperature was $180\text{ }^{\circ}\text{C}$, and the carrier gas was helium with a flow rate of 1 ml min^{-1} . The quantification was obtained by comparison with the reference standard using a MassHunter Workstation (version 10.0; Agilent Technologies Inc.).

Data on ET quantification, expressed as nl g^{-1} FW h^{-1} , represent the mean of three biological replicates, each consisting of a single plant.

2.8. Total RNA extraction, processing and gene expression analysis (RT-qPCR)

The plant transcriptional response was characterized at 12 and 72 h PIT (0, 10 and 30 μM KI) and 48 h PBI, which was performed by inoculating all rosette leaves (1 drop/leaf – Col-0). In the latter case, expression analysis was conducted on mock- and *B. cinerea*-inoculated plants.

To characterize the involvement of iodine in the SA, JA and ET pathways, the transcriptional response of KI-treated Arabidopsis plants was determined on the basis of a pool of genes involved in their biosynthesis, regulation or response. The first group included *SID2*, *PAL1*, *PAL2*, *PAL3*, *PAL4* (SA biosynthesis – Lefevere et al., 2020), *LOX2*, *AOS*, *AOC2* (JA biosynthesis – Wasternack and Hause, 2013) and *ACS*, *ACO1*, *ACO2* (ET biosynthesis – Pattyn et al., 2021). The second group included *SARD1* and *NPR3*, which encode SA transcription factors (Dempsey et al., 2011; Ding et al., 2018), and the third group included several plant defence genes related to the SA (*PR1*, *PR2*, *PR5*) or ET/JA (*PDF1.2*, *PR3*, *PR4*, *PR12*) pathways (Ali et al., 2018; Huffaker, et al., 2006).

Genes involved in a broad spectrum of responses related to abiotic stresses, such as salinity (*DREB2A*, *SOS1*; Park et al., 2016), oxidation (*ZAT12*, *APX1*, Rizhsky et al., 2004) and hypoxia (*ADH1*, Loreti et al., 2018), were also analysed to verify the specificity of iodine in the defence response, excluding its involvement in the activation of a general stress response. After *B. cinerea* inoculation, the expression of *PAD3*, encoding the biosynthesis of the antifungal phytoalexin camalexin (Zhou et al., 1999), was included in the analysis, as it is considered a marker gene for the biotic stress-related response.

Gene expression was determined in shoot and root tissues. Each sample consisted of a pool of rosettes or roots collected from five different plants, which were immediately frozen in liquid nitrogen and stored at -80°C until further analysis.

Total RNA from the rosettes was extracted as described by Perata et al. (1997), whereas RNA from the roots was extracted with Spectrum™ Plant Total RNA Kit (Sigma-Aldrich), according to the manufacturer's instructions. For both tissues, a TURBO DNA-free kit (Thermo Fisher Scientific) was used to remove contaminant DNA, and a Maxima First Strand cDNA Synthesis Kit (Thermo Fisher Scientific) was used for RNA reverse-transcription. Expression analysis was performed by real-time PCR using an ABI Prism 7300 sequence detection system (Applied Biosystems). Quantitative PCR was performed using 33 ng of cDNA and iQTM SYBR® Green Supermix (Bio-Rad Laboratories). Relative expression levels were calculated using the geometric averaging method (GeNorm: <https://genorm.cmgg.be/>), with *UBQ10* as a reference gene. The full list of the primers used and their sequences are reported in Supplementary Table S2.

Real-time PCR analysis was also used to quantify fungal growth on *B. cinerea*-inoculated plants (three days PBI), which was measured as the ratio of the expression of the *Botrytis Actin* gene (*BcActin*) to that of the Arabidopsis *UBQ10* gene.

Three biological replicates and two technical replicates were analysed for all the genes and conditions tested.

2.9. Quantification of hydrogen peroxide (H_2O_2)

Hydrogen peroxide was measured in the leaf and root extracts of Arabidopsis Col-0 plants at 2 and 72 h PIT (0, 10 and 30 μM KI) and 2 h PBI, which was performed on all rosette leaves using six droplets/leaf. The H_2O_2 content was determined using the Amplex® Red Hydrogen Peroxide/Peroxidase Assay Kit (Thermo Fisher Scientific).

A total of 15 plants were used for the assay to generate five biological replicates, each consisting of a pool of 15 detached leaves (one leaf/plant for each replica), or a pool of roots collected from three plants. The H_2O_2 assay was performed on frozen tissues, which were ground to powder and processed according to the manufacturer's instructions. Briefly, each sample (100 mg FW) was mixed with 500 μl of phosphate buffer (50 mM K_2HPO_4 , pH 7.4), and after centrifugation (10,000 rpm for 10 min at 4°C), 50 μl of the supernatant was mixed with 50 μl of working solution consisting of 100 μM Amplex Red reagent and 0.2 U ml^{-1} horseradish peroxidase. The H_2O_2 concentration was quantified on the basis of a calibration curve and determined spectrophotometrically after 30 min of incubation at 37°C in the dark. The fluorescence of the standards and experimental samples (two technical replicates/each) was

read at 545/560 nm (excitation/emission wavelength) by using a microplate reader (Thermo Scientific™ Multiskan™ GO Microplate Spectrophotometer).

In addition, *in situ* H_2O_2 accumulation was determined in fresh samples using 3,3'-diaminobenzidine (DAB) staining. All leaves of KI-treated plants (0, 10 and 30 μM) were analysed at 72 h PIT and 12, 24 and 48 h PBI (two droplets/leaf; six plants/treatment).

Due to the cultivation system used (the hydroponic system) the roots were entangled and thus did not provide clear results in terms of H_2O_2 distribution as a result of the DAB staining. Therefore, we decided to perform this specific quantification on Arabidopsis seedlings grown on vertical plates.

Arabidopsis seeds were sterilized with 70 % ethanol (v/v – 30 s.), washed three times with sterile distilled water, incubated for 6 min with a 20 % NaClO (v/v) solution under agitation and rinsed seven times. A total of 12–13 sterilized seeds were equidistantly sown on 12 cm square vertical plates containing homemade half-strength Murashige & Skoog (MS) media lacking KI (Supplementary Table S3). After two days of vernalization at $+4^{\circ}\text{C}$ in the dark, the plates were placed in a plant incubator set to 25°C with a 12-h photoperiod, a quantum irradiance of 60 $\mu\text{mol photons m}^{-2} \text{s}^{-1}$ and a relative humidity close to 50 %. After seven days of cultivation, the seedlings were gently moved from the iodine-deficient medium to new growth media differing in KI content (0, 10 and 30 μM) and subjected to DAB staining after an additional 72 h of cultivation ($n = 15$). Since *B. cinerea* grows on the aerial part of the plant, the Arabidopsis seedlings were not subjected to fungal inoculation.

The DAB powder (Sigma-Aldrich) was freshly dissolved in H_2O (1 mg ml^{-1}) by acidification with HCl (pH 3.8 with HCl). The plant tissues (leaves/seedlings) were completely immersed in the DAB solution (naturally stabilized at pH 6.8–7), incubated overnight at room temperature and shaken on an oscillator (80–100 rpm) in the dark. After incubation and DAB staining solution removal, the tissues were washed with sodium phosphate buffer (0.1 M, pH 7.2), then bleached in 10 % EtOH solution (v/v) for 10 min at 100°C and subsequently stored in 70 % EtOH solution (v/v) until images were taken. Positive controls were obtained by immersing detached leaves/seedlings which had not been treated with KI nor inoculated with *B. cinerea* in a 35 % H_2O_2 solution (v/v) for 1 h. As an additional positive control, detached leaves of non-inoculated and iodine-untreated plants were subjected to heat stress (1 h at 45°C) before DAB staining.

2.10. Statistical analysis

Data following a normal distribution (Shapiro-Wilk test) and satisfying the assumption of homogeneity of variance (Bartlett's test) were subjected to two-way and/or one-way analysis of variance (ANOVA), followed by Tukey's post-hoc test (95.0 % confidence level). Pairwise comparisons were performed by Student's *t*-test (95.0 % confidence level). Percentage data were analysed via the Kruskal–Wallis test (nonparametric statistic) followed by Dunn's multiple comparison test (95.0 % confidence level). All the statistical analyses were performed using GraphPad Prism (v. 8.0.0 for Windows, GraphPad Software, San Diego, CA, USA).

3. Results

3.1. Effects of iodine on *B. cinerea* growth and pathogenic activity

The effects of iodine (0, 10 and 30 μM KI) on *B. cinerea* growth were characterized *in vivo*, by performing a visual symptom scoring of Arabidopsis leaves at 5 days PBI (Fig. 1).

The plants did not suffer from the addition of iodine to the nutrient solution, as they did not show toxicity symptoms, irrespectively of the KI concentration used (mock, +KI, Fig. 1a). In contrast, the KI treatments strongly increased plant resistance to *B. cinerea* (Fig. 1a). The number of

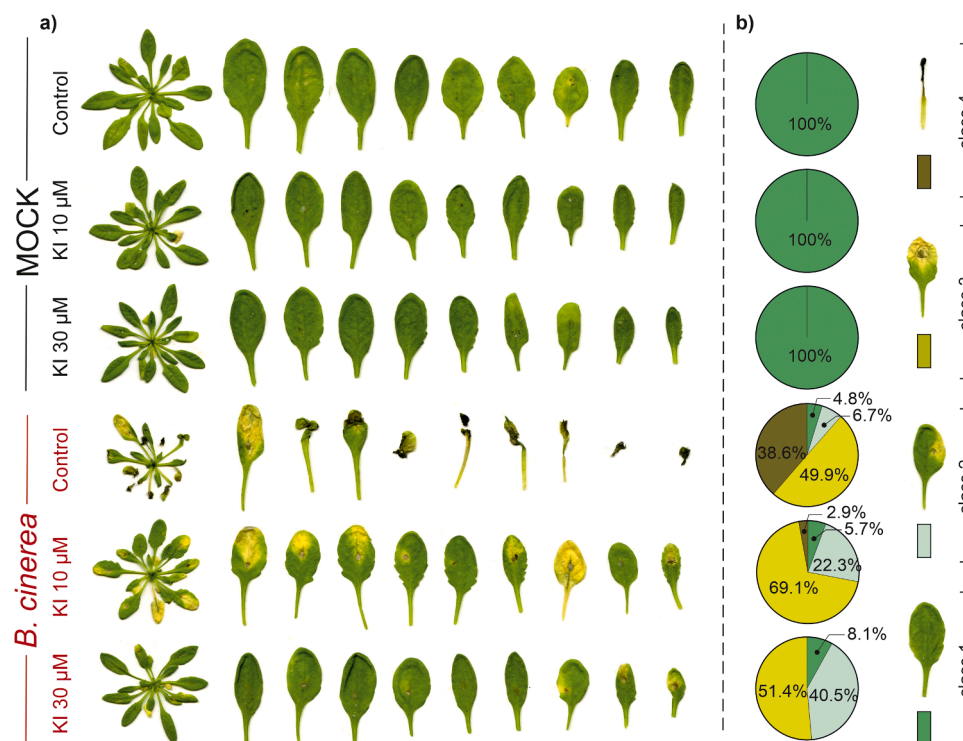


Fig. 1. *In vivo* evaluation of the effect of iodine (0, 10 and 30 μM) against *Botrytis cinerea*. (a) Phenotypes of mock- and *Botrytis*-infected Arabidopsis plants (Col-0) at 5 days post *B. cinerea* infection; all the leaves were inoculated. (b) Pie charts showing the percentages of the different lesion types according to four classes of symptoms: 1, no infection; 2, light browning corresponding to the inoculum droplet; 3, strong browning in the local lesion/yellow leaf; and 4, dark brown/necrotic leaf. The plant phenotype and symptoms were characterized on 15 plants/experimental condition.

class 2 leaves (local lesions/light browning corresponding to the infection site) increased with increasing concentrations of KI (22.3 % and 40.4 % in 10 and 30 μM KI-treated plants, respectively vs 6.7 % of the controls; Fig. 1b, Supplementary Table S4). Conversely, control (KI-untreated) plants were severely affected by the pathogen. In fact, 38.6 % of the leaves belonged to class 4 (most severe symptoms, consisting of dark brown/large necrotic areas), which represented only 2.9 % of the 10 μM KI-treated plants and was completely absent in the 30 μM KI-treated plants (Fig. 1b, Supplementary Table S4). Compared with that in the control plants, the increased proportion of class 3 leaves (intermediate disease level; strong browning in the local lesion/yellow leaf) in the KI-treated plants was due mainly to the reduction in the percentage of class 4 leaves (Fig. 1b, Supplementary Table S4).

At an earlier stage of infection (3 days PBI), the percentage of symptomatic leaves did not differ between the control and KI-treated plants, constituting, on average, 80 % of the total (Fig. 2a). Nevertheless, compared with those of the control plants, the leaf lesion sizes of the 10 and 30 μM KI-treated plants decreased by 26.4 % and 24.6 %, respectively, and the expression level of the *Botrytis-Actin* gene was reduced by 56.6 % and 62.0 %, respectively (Fig. 2a).

At 1 day PBI, the observation of the leaf surface allowed visualization of local browning at the inoculation site, irrespectively of the KI treatment (Fig. 2b). The differences between the treatments became more pronounced over time. At 5 days PBI, the control leaves were completely colonized by the fungus and mostly necrotized, whereas iodine strongly antagonized *B. cinerea* spread, limiting necrotic events, especially in the 30 μM KI-treated plants (Fig. 2b). At 9 days PBI, the pathogen started to sporulate profusely on the dead tissue of the control leaves and minimally on the 10 μM KI-treated leaves, where the conidia were almost limited to the infection site. The fungus never reached the sporulation stage in the 30 μM KI-treated plants (Fig. 2b); the daily progression of fungal growth is reported in Supplementary Fig. S3).

The effect of iodine against *B. cinerea* was also evaluated by removing

the plants from the KI-containing nutrient solution immediately after fungal inoculation (Supplementary Figure S4, Supplementary Table S5). Most of the inoculated leaves pre-treated with KI were scarcely affected by the pathogen and belonged to classes 1 or 2. Conversely, the leaves of control (KI-untreated) inoculated plants were severely damaged by *B. cinerea* and were mainly from class 4. The fungal spread was antagonized by KI treatment in a dose-responsive manner.

To rule out the possibility of a direct biocidal effect of KI against *B. cinerea*, mycelial discs were inoculated *in vitro* on PDA plates supplemented with increasing concentrations of KI (0, 10, 30 and 100 μM). No significant differences were observed in mycelial growth due to iodine treatment (Supplementary Fig. S5a), as also demonstrated by the fungal growth curves, which were almost identical in all the growing media (Supplementary Fig. S5b).

To elucidate the major physiological mechanisms underlying the observed enhanced plant resistance to the pathogen triggered by KI, we performed several biochemical and molecular analyses on plants prior to *B. cinerea* inoculation to evaluate the genuine effect of iodine (pre-infection characterization), and on infected plants, which were pre-treated or not pre-treated with KI (post-infection characterization).

3.2. Pre-infection characterization

3.2.1. Effects of iodine on salicylic acid and jasmonic acid contents, and ethylene production

To investigate the effects of iodine on the accumulation of the key signalling molecules involved in plant resistance to biotic stress, the SA, JA, and ET shoot and root contents were quantified in Arabidopsis (Col-0) plants at 72 h PIT (0, 10 and 30 μM KI; Supplementary Fig. S1). The relatively short-term exposure of plants to KI increased the contents of SA and JA in both shoot (Fig. 3a) and root tissues (Fig. 3b).

In leaves, both signalling molecules were iodine-induced in a dose-responsive manner. Compared with the controls, SA increased by 37

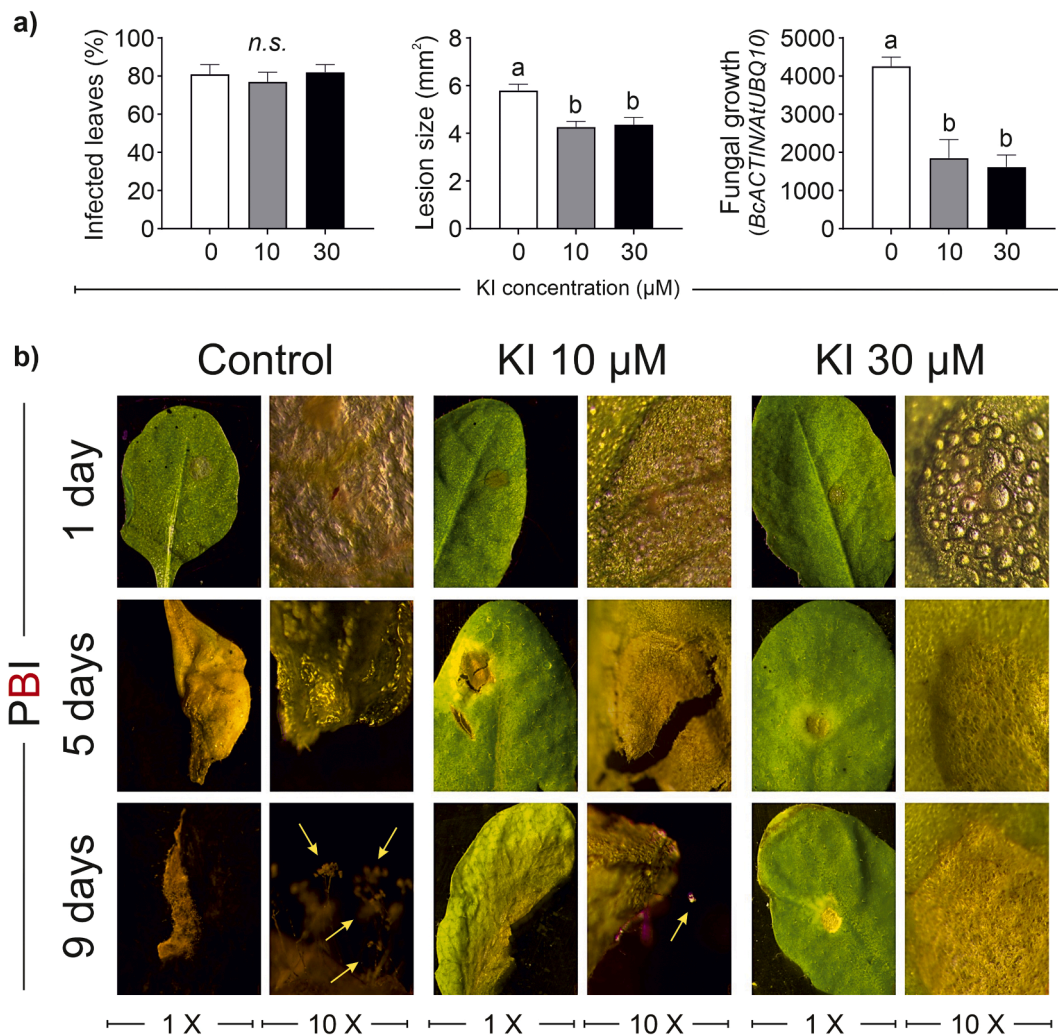


Fig. 2. *Botrytis cinerea*-induced lesion spreading on *Arabidopsis* leaves pretreated with or without iodine (0, 10 and 30 μM KI) 72 h prior to fungal infection. (a) Percentage of symptomatic leaves, lesion size and *B. cinerea* growth (measured by the ratio of *BcActin/AtUBQ10* expression level) determined at 3 days post *B. cinerea* infection (PBI). Morphological determinations were performed on all the leaves of 15 plants/experimental condition, whereas fungal growth was determined on 3 biological replicates, consisting of a pool of 5 plants. The values indicated by different letters significantly differ from each other (according to one-way ANOVA, Tukey's post hoc test, $P \leq 0.05$). n.s.: $P > 0.05$. The error bars are shown in the graphs. (b) Stereomicroscopic observations (1X and 10X magnification scale, $n = 6$) of the lesions at selected days PBI. Conidiophores visualized at 9 days PBI are indicated by yellow arrows.

% in the 10 μM KI-treated plants, and was more than doubled in the 30 μM KI-treated plants, whereas the JA content increased by 12 and 37.6 % (Fig. 3a). In the roots, the increase in SA and JA accumulation was not correlated with the KI concentration used. The SA content in the 10 and 30 μM KI-treated plants was approximately 5- and 4-fold greater than that in the control plants, respectively, whereas the same KI treatments increased JA by 56 % and 19 %, respectively (Fig. 3b).

To verify whether iodine can act as a facilitator of general defence responses in plants, ET production was measured in addition to SA and JA accumulation. A time course experiment was performed to measure the ET emissions of the plants at different time points ranging from 1 to 72 h from the onset of the KI treatments (Fig. 3c). All the plants emitted ET, but whereas the KI-treated plants presented a peak in ET production a few hours after its application, the release of ET was lower and quite constant in the control plants (Fig. 3c). The timing of the ET peak was also affected by the KI concentration used: it was detected early in 30 μM KI-treated plants (2 h PIT), and 8 h PIT in 10 μM KI-treated plants.

3.2.2. Effects of iodine on gene expression

The transcriptional effect of KI treatments was explored in leaf and root tissues sampled at an early stage (12 h PIT) and 72 h after PIT.

The response triggered by KI in the shoot at the mRNA level of selected transcripts was generally less pronounced than that in the roots, especially when the tissues were sampled at 12 h PIT (Fig. 4).

In the shoot, the short application of 30 μM KI (12 h PIT) triggered the expression of the SA-biosynthetic genes *PAL1*, *PAL2* and *PAL3* (Fig. 4a, Supplementary Table S6). Genes related to JA and ET biosynthesis were not affected, apart from *LOX2* and *ACO1*, which were significantly upregulated by 30 μM KI (Fig. 4a; Supplementary Table S6). Neither genes related to SA-regulation (*SARD1* and *NPR3*) nor SA-responsive *PR* genes were affected by KI treatments, whereas *PR3* and *PR4* (JA/ET-responsive genes) were significantly upregulated by the highest KI concentration tested (Fig. 4a, Supplementary Table S6).

At 72 h PIT, iodine preferentially stimulated the expression of genes related to JA biosynthesis (*LOX2*, *AOS* and *AOC2*). ET-biosynthetic genes and SA-biosynthetic genes were not affected by the treatments, with the exception of *PAL2* and *PAL4*, which were downregulated by 30 μM KI (Fig. 4a, Supplementary Table S7).

Iodine clearly stimulated the expression of both SA- and JA/ET-responsive *PR* genes, more than doubling the expression of *PR2* and *PR5* (SA-responsive), and *PR3* and *PR4* (JA/ET-responsive) compared with that of the controls. These genes were particularly induced by 30

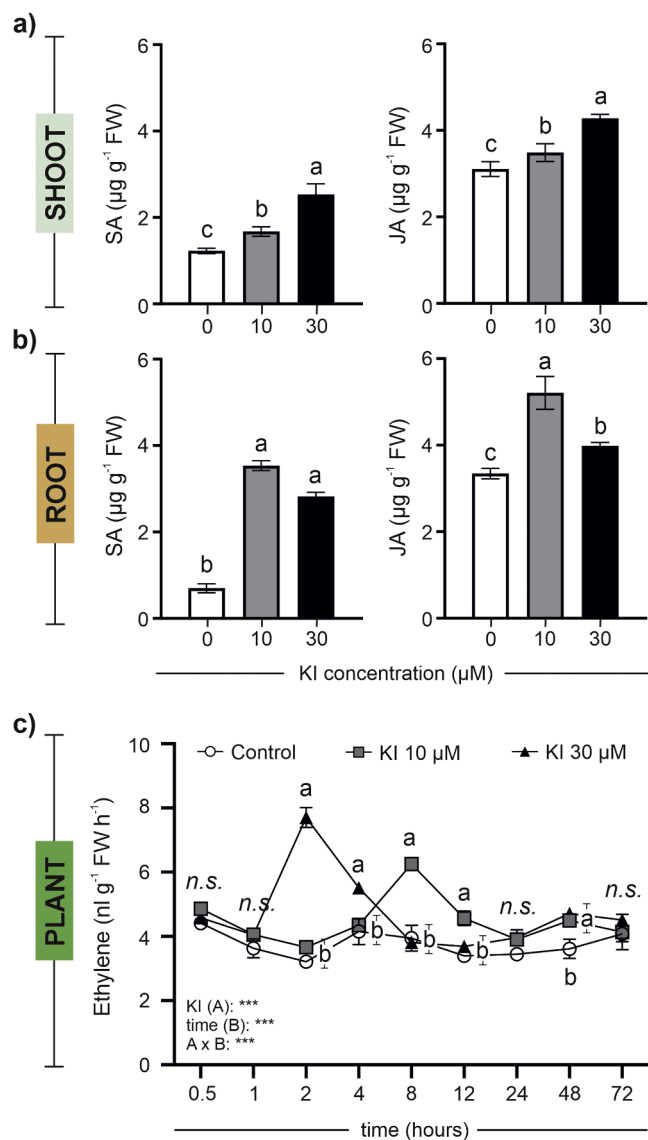


Fig. 3. Effects of iodine (0, 10 and 30 µM KI) on salicylic acid (SA), jasmonic acid (JA) and ethylene (ET) accumulation/release. Shoot (a) and root (b) SA and JA contents quantified at 3 days post iodine treatment (PIT). The data are the means of three replicates, each consisting of a pool of samples derived from 5 plants. (c) Plant ET release measured at different time points following the onset of iodine treatment ($n = 3$). The values indicated by different letters significantly differ from each other (according to one-way ANOVA, Tukey's post hoc test, $P \leq 0.05$). Statistical analysis of ET release was conducted at each time point. Error bars are shown.

µM KI (Fig. 4a, Supplementary Table S7). None of the abiotic stress-related genes were significantly affected by KI, irrespective of the duration of the treatment (12 h or 72 h PIT) or the KI concentration used (Fig. 4a, Supplementary Tables S6, S7).

In roots, KI rapidly (12 h PIT) triggered the activation of SA biosynthetic genes (*SID2*, *PAL1*, *PAL2* and *PAL3*) and SA transcription factors (*SARD1* and *NPR3*), together with the downregulation of SA-responsive PRs (*PR1*, *PR2* and *PR5*), irrespectively of the KI concentration used (Fig. 4b, Supplementary Table S8). In contrast, genes involved in JA or ET biosynthesis were scarcely affected by KI or even downregulated (*LOX2*, *AOC2* and *ACO2*), whereas JA/ET-responsive PRs (*PR3*, *PR4* and *PR12*) were induced by 10 and/or 30 µM KI (Fig. 4b, Supplementary Table S8).

A very different transcriptional response was observed later (72 h PIT). In fact, genes related to SA biosynthesis were downregulated by KI

treatments (*PAL1*, *PAL2*, and *PAL4*), whereas there was a very strong upregulation of SA-responsive PRs (Fig. 4b, Supplementary Table S9). In particular, the expression of *PR1* was approximately 300 to 1400-fold higher than that of the controls in 10- and 30-KI-treated plants, respectively, and was approximately 1000 to 6100-fold higher in the case of *PR5* (Supplementary Table S9). In addition, the JA/ET responsive genes *PR3* and *PR4* were downregulated by KI treatments (Fig. 4b, Supplementary Table S9).

The transcription of abiotic stress-related genes, which were used as controls to assess the possible impact of iodine on pathways unrelated to biotic stress responses, was not univocally regulated by the KI treatments. *ZAT12*, *ADH* and *DREB2A* were upregulated by 30 µM KI at both sampling times (12 h and 72 h PIT), whereas *APX1* and *SOS1* were not affected by the treatments (Fig. 4b, Supplementary Tables S8, S9).

3.3. Post-infection characterization

3.3.1. Effects of iodine on salicylic acid and jasmonic acid contents and ethylene production in the presence/absence of *Botrytis cinerea* infection

The experiments described in the previous subsections demonstrated the positive role of iodine in SA and JA accumulation in both the shoots and roots (Fig. 3a, b) of healthy plants (Fig. 1) and revealed how iodine regulates the timing and amount of ET released from the whole plant (Fig. 3c). The quantification of the three hormones was then repeated on *B. cinerea*-inoculated Col-0 plants, which were cultivated in nutrient solution with or without KI (0, 10 and 30 µM KI) (Fig. 5).

The SA and JA quantifications were performed on leaf and root tissues sampled at 5 days PBI (8 days PIT), once symptoms were already present on the plants. ET emissions were determined for the whole plant at 1, 2 and 3 h PBI, which resulted in the optimal time window for sampling, as we demonstrated that *B. cinerea* induced a peak of ET emission at 2 h PBI (Supplementary Figure S6).

In the absence of the pathogen (mock plants), KI had no clear effect in terms of SA and JA accumulation in the shoot (Fig. 5a) and did not alter plant ET emission (Fig. 5c). Nevertheless, 30 µM KI stimulated SA accumulation in the roots, which was approximately 11-fold greater than that of the controls, and reduced JA accumulation by approximately 4-fold (Fig. 5b).

In the absence of iodine (0 µM KI or control), the shoot SA content did not differ between mock- and *B. cinerea*-infected plants (Fig. 5a). On the other hand, *B. cinerea* triggered JA accumulation in the shoot (the part of the plant of interest for fungal growth), which was up to 6-fold higher than that of the mock control samples (Fig. 5a).

In iodine-untreated roots, the SA and JA contents of *B. cinerea* infected plants were almost doubled and halved, respectively, compared with those of their related mock plants (Fig. 5b).

In the presence of iodine, *B. cinerea*-inoculated plants accumulated more SA and less JA in the shoot than did their related controls (0 µM KI – *B. cinerea*-inoculated plants) (Fig. 5a). Specifically, the SA content of *B. cinerea*-inoculated plants treated with 10 and 30 µM KI was 5- and 2-fold higher than that of the control, respectively, whereas JA content was reduced on average >3-fold (Fig. 5a). In roots, the SA and JA contents of *B. cinerea*-inoculated plants was not affected by KI treatments (Fig. 5b). Iodine-treated plants also produced less ET than the controls did, as demonstrated by the flattening of the *B. cinerea*-induced ET emission peak observed at 2 h PIT (–34% and –20% compared with the controls in 10 and 30 µM KI-treated plants, respectively – Fig. 5c).

3.3.2. Iodine effect on gene expression in the presence/absence of *Botrytis cinerea* infection

To gain insight into the effects of iodine and *B. cinerea* on defence-related gene expression, the transcriptional response of the previously selected genes (Fig. 4) was analysed in Col-0 shoots and roots sampled at 48 h PBI (corresponding to 5 days PIT) (Fig. 6). The expression of *PAD3*, involved in the biosynthesis of the antifungal phytoalexin camalexin, was included in the analysis.

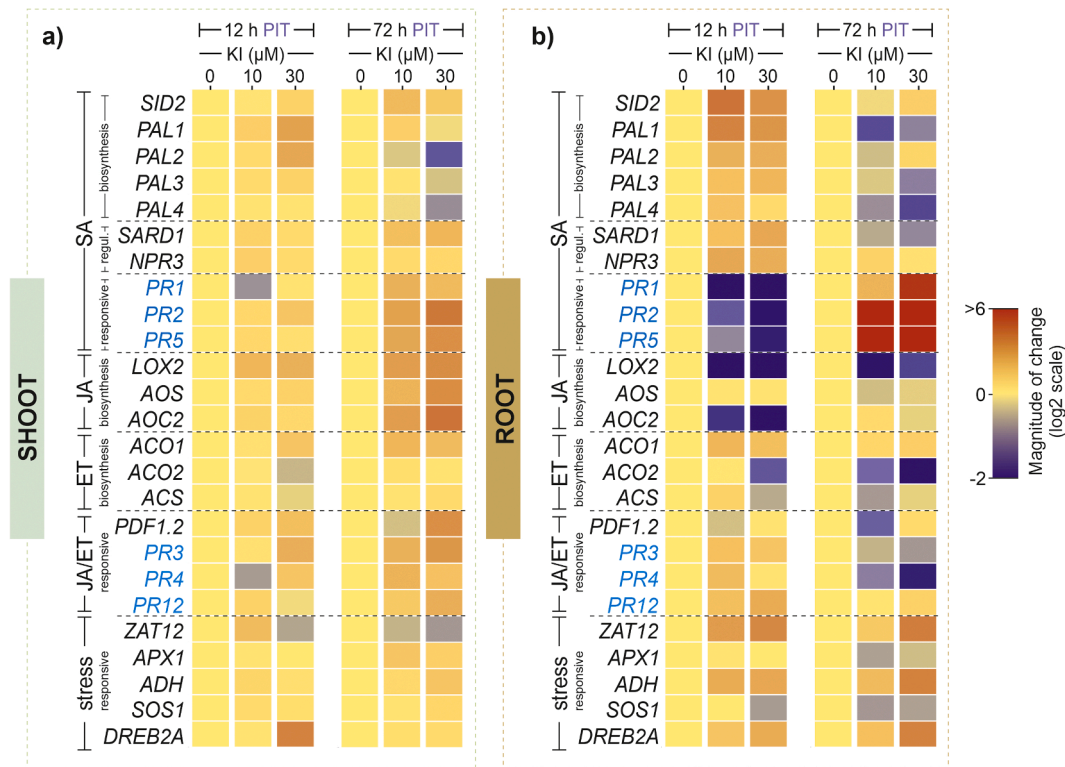


Fig. 4. Transcriptional regulation triggered by iodine treatments (0, 10, and 30 μM KI). Heatmap showing the relative expression levels of selected genes related to salicylic acid (SA), jasmonic acid (JA) and ethylene (ET) biosynthesis/signalling or as markers of biotic and abiotic stress. Determinations were performed on shoot (**a**) and root (**b**) tissues at 12 h post iodine treatment (PIT) and 72 h PIT (reference: iodine-untreated tissues). The numerical expression values and statistical significance are shown in Supplementary Tables S6, S7, S8, and S9. The data are the means of three biological replicates, each consisting of a pool of samples derived from 5 plants. Two technical replicates were included in the analysis.

In shoots, the transcriptional response was strongly affected by the presence of *B. cinerea* and far less influenced by KI treatments (Fig. 6a, Supplementary Table S10). Except for *PR5* (Supplementary Table S10), fungal infection positively affected the expression of all the analysed genes, whereas iodine significantly affected the expression of a small group of genes, particularly the SA-responsive *PR2* and *PR5* genes (Fig. 6a, Supplementary Table S10). In mock-treated plants, the expression of *PAD3* and *ZAT12* decreased with increasing KI. The two genes were strongly activated by *B. cinerea*, although both 10 and 30 μM KI significantly reduced the expression of *ZAT12* compared with that of its related control (Fig. 6a, Supplementary Table S10).

Compared with that of the shoots, the transcriptional response of the roots was almost the opposite, as it was scarcely influenced by the presence of *B. cinerea* (Fig. 6b, Supplementary Table S11), and largely mirrored that observed at 72 h PIT due to KI-treatments (Fig. 4b). In both mock-treated and inoculated plants, the expression of genes related to JA and ET biosynthesis was scarcely affected or downregulated by 10 and 30 μM KI, with the exclusion of *SID2*, which was induced by KI treatments (Fig. 6b, Supplementary Table S11). Iodine triggered the activation of *PR2* and *PR5* (SA-responsive genes), and that of *PR3* and *PR4* (JA/ET-responsive genes), although to a lesser extent. Iodine clearly induced *PAD3* expression, irrespectively of the concentration used, whereas *ZAT12* was significantly activated by 30 μM KI (Fig. 6b; Supplementary Table S11).

3.4. Effects of iodine on plant redox homeostasis and hydrogen peroxide (H_2O_2) accumulation in the presence/absence of *Botrytis cinerea*

To explore the possible role of iodine in H_2O_2 metabolism, which is involved in the plethora of physiological mechanisms associated with plant resistance against biological attacks (Saxena et al., 2016; Smirnov and Arnaud, 2019), the shoot and root H_2O_2 contents were determined

in KI-treated plants (0, 10 and 30 μM - Col-0) sampled at 2 h and 72 h PIT and immediately after *B. cinerea* inoculation (2 h PBI; Fig. 7a).

Iodine feeding did not alter the shoot or root H_2O_2 content after a short exposure time (2 h PIT; Fig. 7a). Conversely, 30 μM KI significantly affected H_2O_2 accumulation at 72 h PIT, which exceeded 50 % of that of the control in the shoot and was almost doubled in the root (Fig. 7a).

In contrast, KI appeared to prevent H_2O_2 accumulation in the shoots of *B. cinerea*-infected plants, as the contents of 10 and 30 μM KI were 57 % and 86 % lower than those of the control, respectively (Fig. 7a), reaching values well below those recorded before fungal infection.

The presence of the pathogen did not affect H_2O_2 accumulation in the roots, whose content was stimulated by 30 μM KI (Fig. 7a).

The H_2O_2 levels after *B. cinerea* infection correlated well with *ZAT12* transcriptional activity (Fig. 7b). Increasing KI concentrations progressively decreased the expression of *ZAT12* in the shoot, whereas 30 μM KI significantly promoted its expression in the root compared with that of the control.

The DAB staining assay performed on detached leaves at 72 h PIT and after *B. cinerea* infection (12, 24 and 48 h PBI) did not reveal differences in terms of H_2O_2 accumulation due to KI treatments (Fig. 7c). A similar response was also observed in the root tissues of Arabidopsis seedlings sampled at 72 h PIT (Fig. 7d).

3.5. Effects of iodine on the tolerance of salicylic acid- jasmonic acid- and ethylene-mutants when challenged with *Botrytis cinerea*

To elucidate the role of SA, JA and ET in the iodine-induced plant defence response, we tested the effect of KI treatment (0 or 30 μM) on Arabidopsis mutants impaired in SA, JA or ET biosynthesis/signalling and infected with *B. cinerea* (Supplementary Figure S7). The tolerance experiment previously described for Col-0 was performed using *sid2-3*, which is defective in SA biosynthesis (Pluhařová et al., 2019), *jar1-1*,

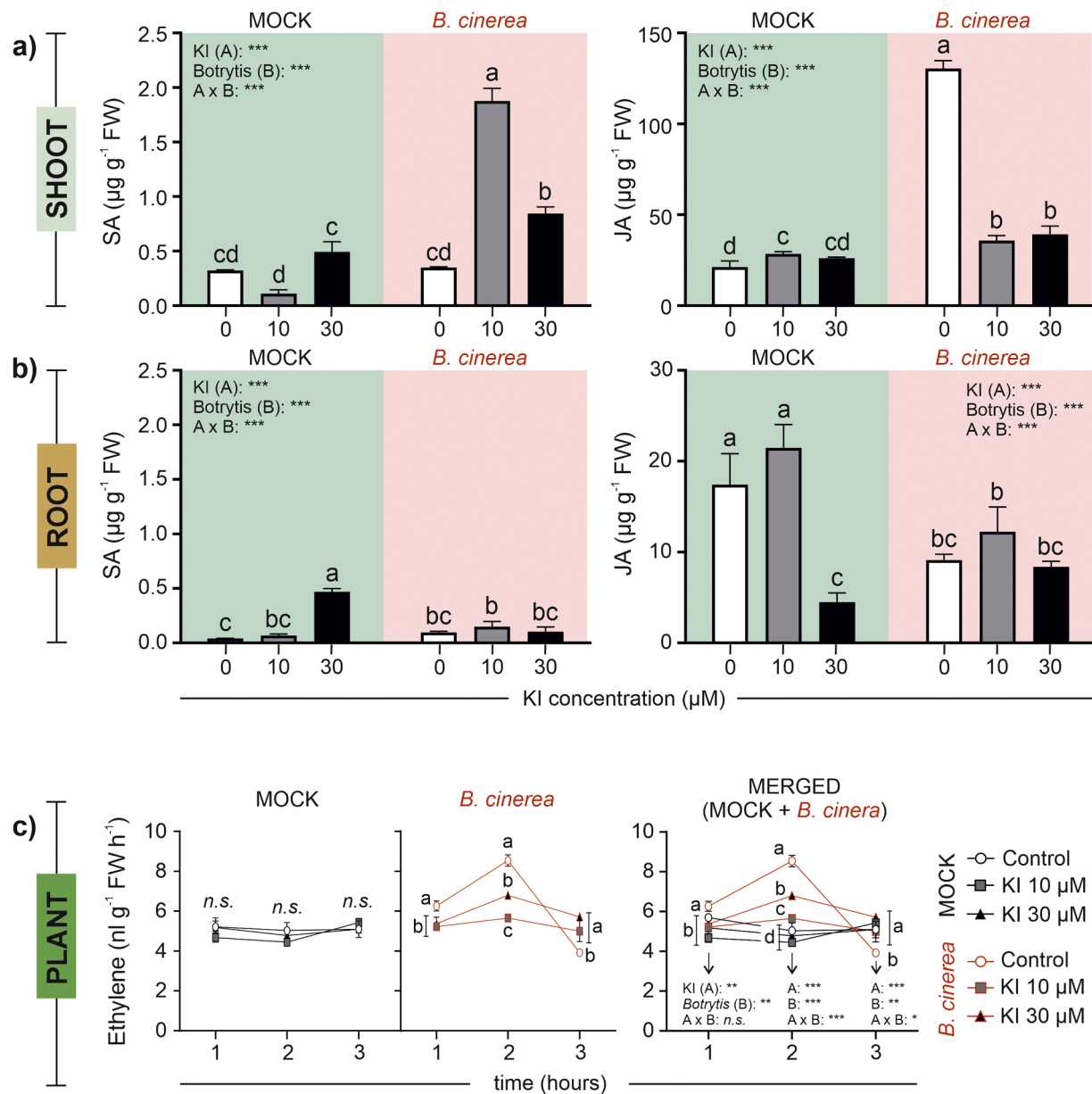


Fig. 5. Effects of iodine (0, 10, and 30 µM KI) on salicylic acid (SA), jasmonic acid (JA) and ethylene (ET) accumulation/release in *Arabidopsis* plants (Col-0) infected with *Botrytis cinerea*. Non-infected plants (mock) were included in the analysis. (b) SA and JA contents quantified at 5 days post *B. cinerea* infection (PBI). The data are the means of three replicates, each consisting of a pool of samples derived from 5 plants. (c) Plant ET release measured at different time points following *B. cinerea* inoculation ($n = 3$). The data were subjected to two-way and one-way analysis of variance (ANOVA). The significance of the two-way ANOVA results is reported in the graphs. The values indicated by different letters significantly differ from each other (according to one-way ANOVA, Tukey's post hoc test, $P \leq 0.05$). Statistical analysis of ET release was conducted at each time point. Error bars are shown.

which is defective in JA signalling (Staswick et al., 1992), and *acs2-1acs6-1*, which is defective in ET biosynthesis (Tsuchisaka et al., 2009) (Supplementary Figure S8).

All the genotypes were affected by *B. cinerea* infection, although *sid2-3* plants presented a good degree of tolerance, even in the absence of iodine (Fig. 8a, b). The sum of leaves belonging to class 1 and class 2 (healthier leaves) indicated that KI treatment increased resistance to the pathogen in the Col-0 and *acs2-1acs6-1* genotypes but did not affect resistance in the *sid2-3* and *jar1-1* genotypes (Fig. 8c). While the lack of iodine effects on *sid2-3* was due to their intrinsic high tolerance to *B. cinerea*, the response of *jar1-1* was comparable to that of the wild type in the absence of iodine, with the latter failing to induce tolerance when applied.

4. Discussion

Brown et al. (2022) redefined the term “plant nutrient” as follows: A mineral plant nutrient is an element which is essential or beneficial for plant growth and development or for the quality attributes of the harvested product of a given plant species grown in its natural or cultivated environment. A plant nutrient may be considered essential if the life cycle of a diversity of plant species cannot be completed in the absence of the element. A plant nutrient may be considered beneficial if it does not meet the criteria of essentiality, but can be shown to benefit plant growth and development or the quality attributes of a plant or its harvested product.

Considering this new definition, iodine is considered a plant nutrient (Brown et al., 2022). Plant nutrients play a crucial role in plant protection against biotic attacks (Tripathi et al., 2022). Therefore, as a

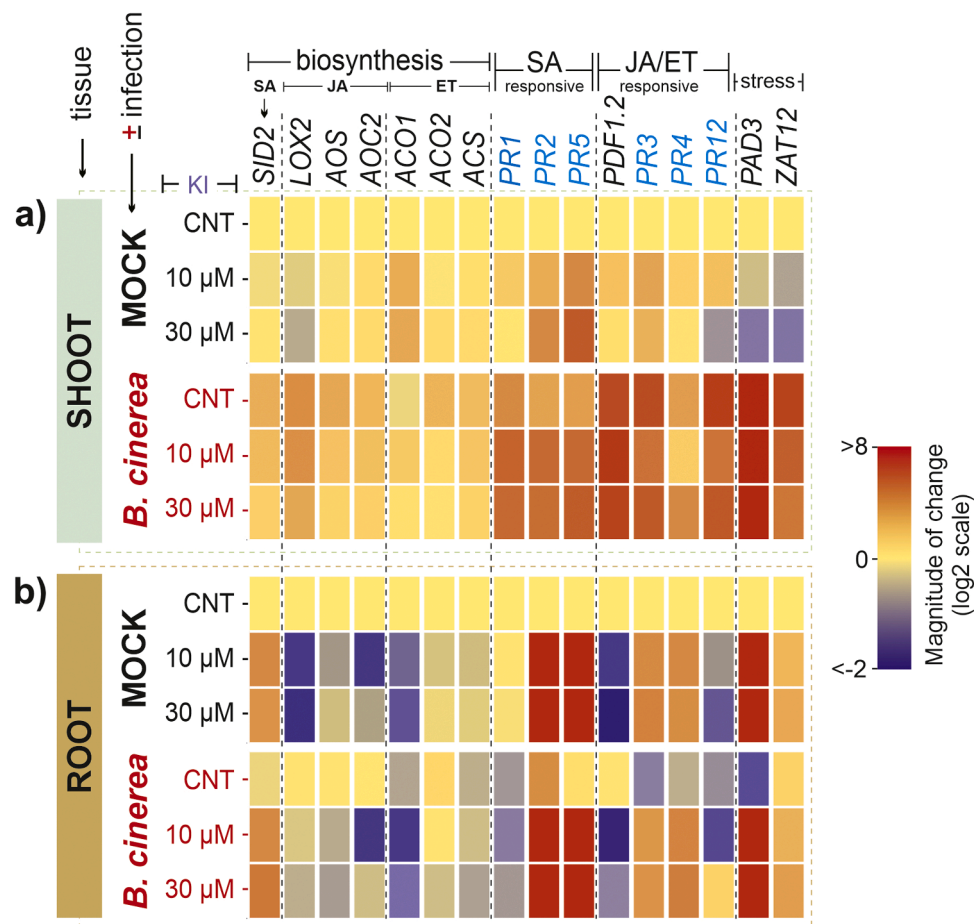


Fig. 6. Transcriptional regulation triggered by iodine (0, 10, and 30 μ M KI) in Arabidopsis plants (Col-0) infected with *Botrytis cinerea*. Non-infected plants (mock) were included in the analysis. Heatmap showing the relative expression levels of selected genes related to salicylic acid (SA), jasmonic acid (JA) and ethylene (ET) biosynthesis/signalling or as markers of biotic and abiotic stress. Determinations were performed on shoot (a) and root (b) tissues at 48 h post *B. cinerea* infection (PBI) (reference: iodine-untreated tissues-mock plants). The numerical expression values and statistical significance are shown in Supplementary Tables S10 and S11. The data are the means of three biological replicates, each consisting of a pool of samples derived from 5 plants. Two technical replicates were included in the analysis. CNT = control: iodine-untreated samples.

modern “physiological” syllogism, we might conclude that iodine could play a role in plant protection against biotic attacks.

The direct evidence of the protective role of iodine against biotic attacks in plants is missing (Riyazuddin et al., 2023). Then, to validate our deduction, we initially demonstrated that iodine treatments protected Arabidopsis plants against the necrotrophic fungus *B. cinerea*, and that a comparable degree of protection was achieved both in the continuous presence of iodine (KI was maintained both in the solution until the end of the trial; Fig. 1, Supplementary Table S4) and by removing iodized salt immediately after pathogen inoculation (Supplementary Figure S4, Supplementary Table S5).

We found that iodine limited fungal spread but did not prevent plant infection (Fig. 2). The *Botrytis cinerea* pathogenic process occurs in three phases: (1) appressorium-mediated penetration of the host cuticle, (2) the formation of local necrotic lesions and fungal biomass accumulation, and (3) a late phase involving lesion spread and sporulation (Bi et al., 2023; Cheung et al., 2020).

The first stage of pathogenesis was not affected by iodine, as local lesions were present at the site of inoculation of both the control and KI-fed plants (Fig. 2b), involving the same percentage of leaves (Fig. 2a). However, the protective action of iodine became increasingly evident over time. At 3 days PIT, we observed a significant reduction in fungal growth (Fig. 2a) and a decrease in the size of the related fungal lesions (Fig. 2a). Towards the end of the trial, the KI-treated plants, especially the 30 μ M-fed plants, were only marginally affected by the presence of

the fungus, which in contrast generally reached the sporulation phase in the control plants, with total necrotization of the leaf tissues (Fig. 2b, Supplementary Fig. S3).

Once the antifungal activity of KI had been excluded *in vitro* (Supplementary Figure S5), we investigated the possible physiological mechanisms triggered by iodine at the basis of the acquired plant tolerance observed *in vivo*. We focused on the main mechanisms involved in the plant pathogenic response, such as the accumulation of SA, JA and ET, which are the three major hormonal players (Ding et al., 2022), the transcriptional response of selected genes related to their biosynthesis or signalling, and the H_2O_2 accumulation, due to its dual role in plant metabolism, acting both as oxidative and signalling molecule during biotic-stress responses (Saxena et al., 2016; Smirnov and Arnaud, 2019).

In the absence of the pathogen (pre-infection characterization), we found that iodine promoted the accumulation of SA and JA in shoots and roots (Fig. 3a, b) and stimulated plant ET release within a relatively short time (72 h PIT - Fig. 3c).

From a transcriptional point of view, plants responded to iodine treatments by modulating the SA, JA and ET pathways, affecting the expression of both biosynthetic and signalling-related genes to a different extent depending on the gene and tissue analysed, the time of KI exposure (12 h, 72 h) and the KI concentration used (Fig. 4). Nevertheless, the genes most responsive to iodine treatments were those encoding PR proteins, which play crucial roles in plant resistance against

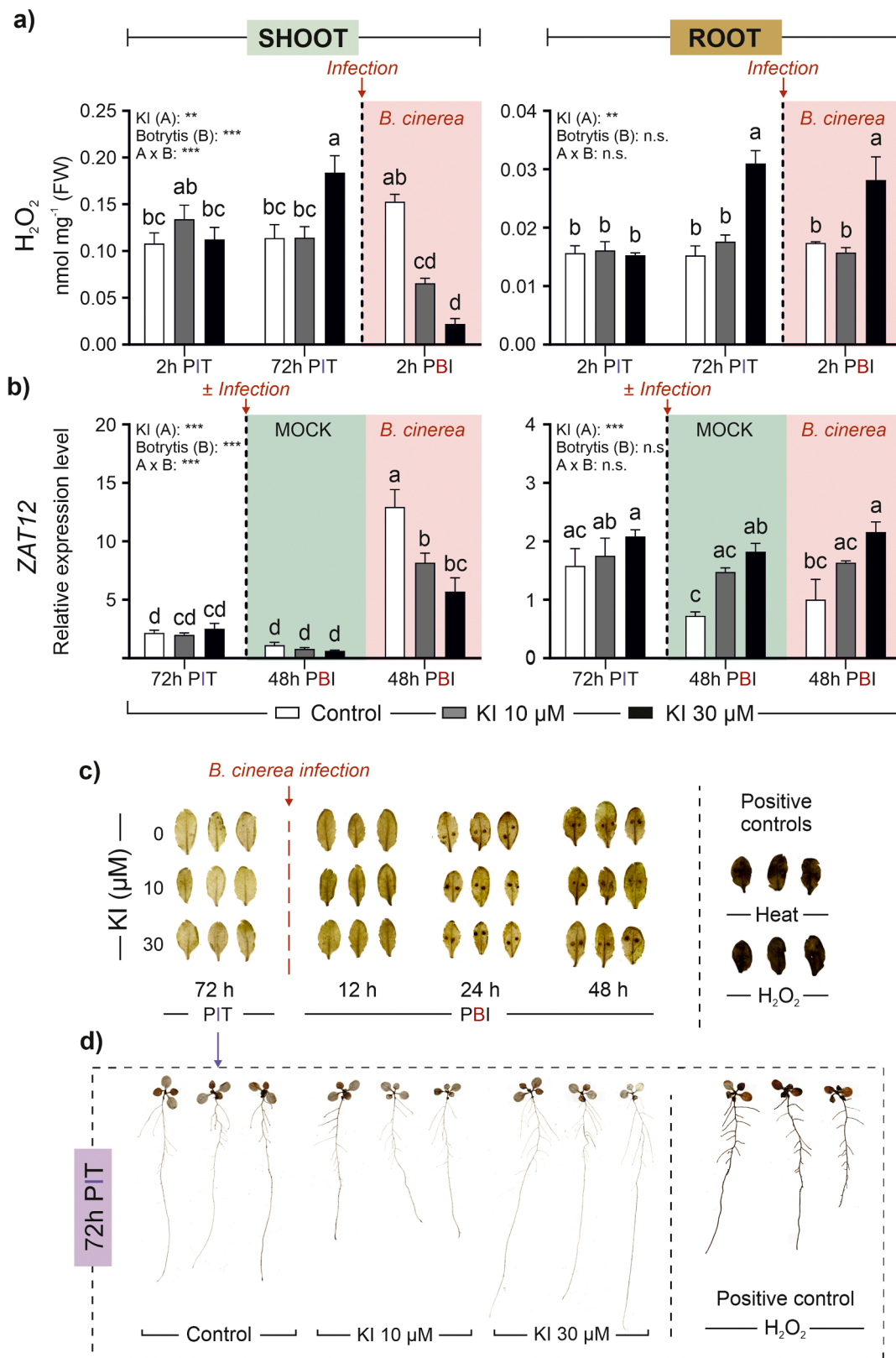


Fig. 7. Effects of iodine (0, 10 and 30 μM KI) on the oxidative status of *Arabidopsis* (Col-0) plants. Non-infected plants (mock) were included in the analysis. Shoot and root hydrogen peroxide (H₂O₂) content ($n = 5$) (a) and *Zat12* expression levels ($n = 3$) (b). The data were subjected to two-way and one-way analysis of variance (ANOVA). The significance of the two-way ANOVA results is reported in the graphs. The values indicated by different letters significantly differ from each other (according to one-way ANOVA, Tukey's post hoc test, $P \leq 0.05$). Error bars are shown. *In situ* H₂O₂ accumulation was characterized in (c) detached leaves (all the leaves from 6 plants) and (d) *Arabidopsis* seedlings ($n = 15$) via 3,3'-diaminobenzidine (DAB) staining. PIT: post iodine treatment. PBI: post *B. cinerea* infection.

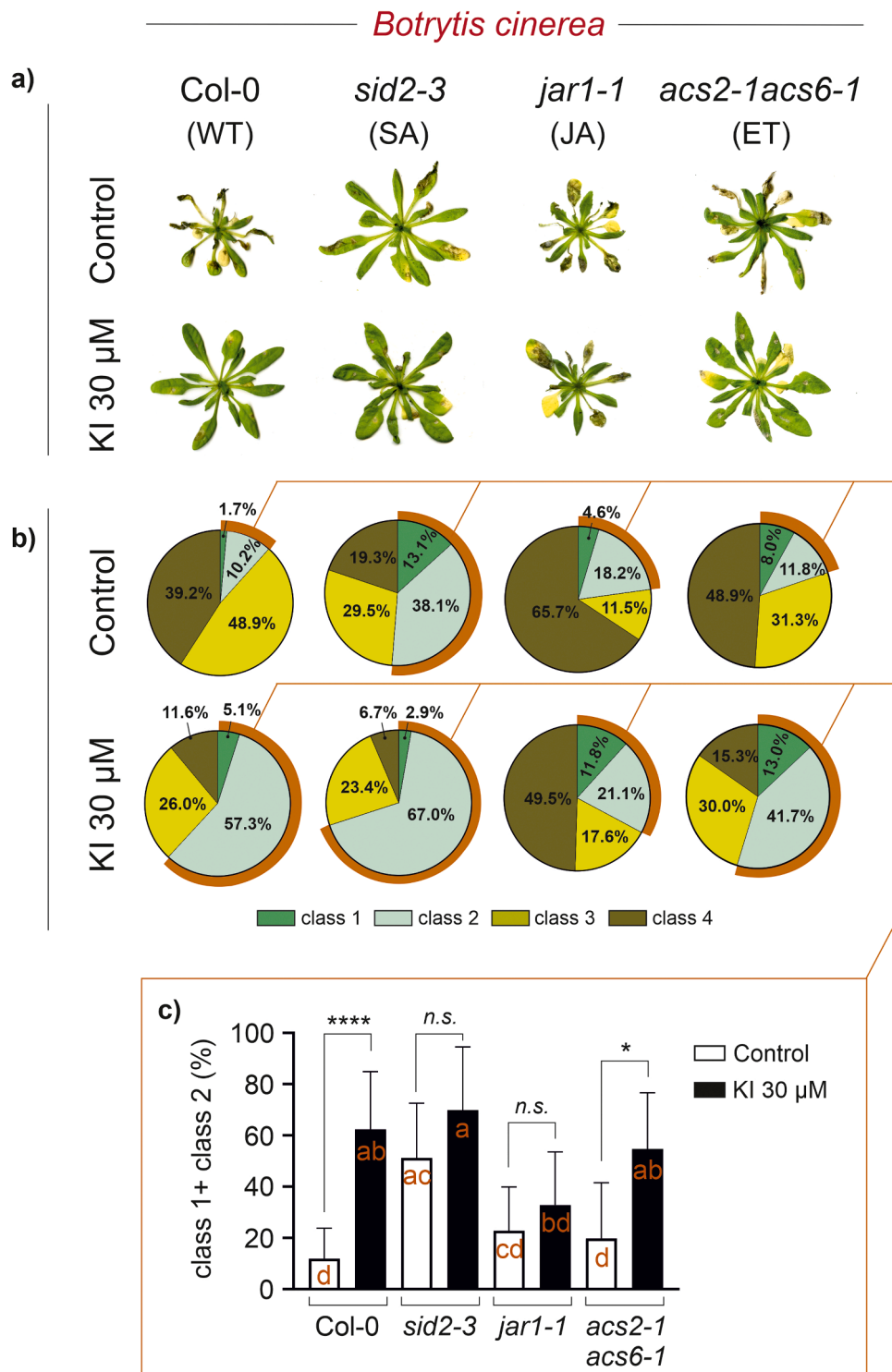


Fig. 8. The protective role of iodine (0 and 30 μM KI), against *Botrytis cinerea* in wild-type (Col-0) Arabidopsis and the following mutants: *sid2-3* [defective in salicylic acid (SA) biosynthesis], *jar1-1* [defective in jasmonic acid (JA) signalling] and *acs2-1acs6-1* [defective in ethylene (ET) biosynthesis]. **(a)** Plant phenotype at 5 days PBI (post *B. cinerea* infection, all the leaves were inoculated). **(b)** Pie charts showing the percentages of the different lesion types according to four classes of symptoms: 1, no infection; 2, light browning corresponding to the inoculum droplet; 3, strong browning in the local lesion/yellow leaf; and 4, dark brown/necrotic leaf. **(c)** Plant tolerance degree expressed as the percentage of leaves belonging to less severe classes of symptoms (class 1 + class 2). The data were analysed via the Kruskal–Wallis test (non-parametric statistic) followed by Dunn’s multiple comparison test (95.0 % confidence level). Medians with different letters differ significantly ($n = 15$). Significant differences between control and KI-treated plants within each genotype are labelled with an asterisk (n.s. $P > 0.05$; * $P \leq 0.05$; ** $P \leq 0.005$; *** $P \leq 0.0005$; **** $P \leq 0.0001$). Standard deviations are shown.

fungal pathogens by preventing or limiting their invasion and spread. Unlike their structures and activities, PR proteins can deteriorate the structure and functionality of several fungal components, including the cell wall, the plasma membrane and several intracellular targets, such as ribosomes, thus altering protein synthesis and, in turn, the fate of fungal cells. Several plant peroxidases are also classified among the PR protein families, as they can contribute to plant cell wall reinforcement by promoting lignification and callose deposition, leading to enhanced resistance against pathogens and stimulating the synthesis of signal molecules involved in plant defence, such as H₂O₂ (Ali et al., 2018; Dos Santos and Luiz Franco, 2023).

In our trial, KI treatments particularly stimulated the expression of the SA-responsive *PR2* and *PR5* genes (Fig. 4), which encode for the β -1,3 glucanase enzyme, which is involved in fungal cell wall degradation (Ali et al., 2018; Dos Santos and Luiz Franco, 2023), and for a thaumatin-like protein, which impairs the fungal plasma membrane through the formation of transmembrane pores (Ali et al., 2018; Dos Santos and Luiz Franco, 2023). We found that KI induced the expression of some abiotic stress-responsive genes in the root (Fig. 4b), which is the entry point for iodine, as KI was added to the plant nutrient solution. In particular, KI triggered the up-regulation of *ZAT12* (72 h PIT; Fig. 7b, Fig. 4b, Supplementary Table S9), which is involved in reactive oxygen and abiotic stress signalling (Davletova et al., 2005). This up-regulation correlated well with the increased H₂O₂ content quantified in the roots, but also in the shoots of the KI-treated plants at 72 h PIT (Fig. 7a).

Like any chemical compound or nutrient, iodine can result in phytotoxic effects when applied at high concentrations, especially in the iodide form, leading to an over-accumulation of reactive oxygen species (ROS) and related cellular damage (Zhang et al., 2023).

Iodine does not appear to act as a generic abiotic stress agent for plants on the basis of three observations in our experiments: 1. The effective concentrations of KI in the nutrient solution used were in the micromolar range. 2. KI did not activate the transcriptional response of abiotic stress marker genes in the shoot (e.g., *APX1*, *ADH*, *SOS1*; Fig. 4a). 3. DAB staining performed at 72 h PIT did not reveal any differences in terms of H₂O₂ accumulation in the leaves or roots of Arabidopsis plants or seedlings (Fig. 7c, d).

Considering the central role of H₂O₂ as a signalling molecule and the fine-tuned balance between H₂O₂ production and scavenging that is required to maintain H₂O₂ levels under the toxicity threshold (Hossain et al., 2015), the increased H₂O₂ content induced by KI (spectrophotometrically determined - Fig. 7a), together with the upregulation of *ZAT12* (Fig. 7b), would seem to be related to its role as a secondary messenger rather than a consequence of oxidative stress.

All the described processes due to KI treatments induced systemic plant immunity because KI was administered to the roots and exerted a protective action on the aerial part of the plant, which is the one associated with *B. cinerea* infection.

In general, the systemic immune response triggered by necrotrophic pathogens is mainly mediated by JA and ET, whereas the SA pathway is stimulated against biotrophic and hemi-biotrophic pathogens (Vlot et al., 2021). In both the cases, once a biotic stimulus has been perceived, plants trigger massive transcriptional reprogramming, which typically results in the upregulation of PR genes and leads to the production of antimicrobial secondary metabolites, such as phytoalexins. In addition, plants respond to pathogenic attacks by increasing the production of reactive oxygen species (ROS), including H₂O₂ (Jung and Cecchini, 2023). All these responses resemble those induced by iodine in the present study.

Another common and key phenomenon of the plant systemic immune response is defence priming, which consists of a physiological state induced in plants pre-experienced with biotic agents, allowing them to respond more rapidly and/or efficiently to subsequent pathogen attacks (Hönig et al., 2023; Jung and Cecchini, 2023). Together with biotic agents, systemic resistance and priming can be triggered by the exogenous application of chemicals, which may activate the plant

immune response due to structural similarity with natural biotic elicitors or irrespective of that (Hönig et al., 2023; Zhou and Wang, 2018). Our data collected after *B. cinerea* infection suggest a genuine role of iodine in plant priming against biotic stresses.

With respect to the three hormones playing a predominant role in plant pathogen resistance, in the absence of disease pressure (mock plants), prolonged (8 days) plant exposure to KI did not result in increased accumulation of SA and JA in the shoot compared with the control (Fig. 5a) and did not affect plant ET release over a period of three hours following 72 h pre-inoculation (Fig. 5c). The transcriptional data corroborated these findings. In fact, the genes related to SA, JA and ET biosynthesis in samples from mock plants were essentially unaffected by prolonged KI exposure in the shoot (Fig. 6a). Nevertheless, significant upregulation of the SA-related *PR2* and *PR5* genes was observed in response to KI treatment (Fig. 6a; Supplementary Table S10).

In the presence of the pathogen, the major hormonal responses occurred in the shoot, which is the part of the plant of interest for fungal growth, as also highlighted by the broad transcriptomic rearrangement observed in this tissue compared with mock and *B. cinerea*-infected tissues (Fig. 6a; Supplementary Tables S10).

Plant defences activated against necrotrophic pathogens, such as *B. cinerea*, are mainly mediated by the JA and ET signalling pathways (Vlot et al., 2021; Li et Cheng, 2023). Therefore, the notable induction of JA in infected control shoots (place of infection - Fig. 5a), as well as that of ET (quantified in the whole plant - Fig. 5c), was expected.

The shoot JA content of *B. cinerea*-infected plants, treated with KI, was much lower than that of their controls (*B. cinerea*-infected, KI-untreated plants; Fig. 5a), and a similar response was observed in terms of ET release (Fig. 5c). These findings suggest that KI-treated plants were scarcely induced to activate JA- and ET-mediated defence responses, as the presence of the pathogen was strongly restrained in this group of plants (Fig. 1). In contrast, plants pre-experienced with iodine were induced to accumulate higher levels of SA in the shoot than were observed in the controls (Fig. 5a), possibly because of the memory (Oberkofler et al., 2021) of the initial application of KI, which was perceived by the plant as a stimulus triggering IR-like responses (pre-infection characterization).

The shoots of *B. cinerea*-infected plants treated with KI had a lower H₂O₂ content than those of the control plants (Fig. 7a). This finding correlated well with the dampening of *ZAT12* expression levels observed in KI-treated plants (Fig. 7b; Fig. 6a; Supplementary Table S10), suggesting that iodine treatments are able to limit the occurrence of pathogen-driven oxidative stress.

Roots were not affected by *B. cinerea* infection. Consequently, the transcriptional profiles in this tissue were unrelated to the presence/absence of the pathogen, as they were almost identical in mock-infected and *B. cinerea*-infected plants and fully dependent on KI treatments (Fig. 6b; Supplementary Tables S11). Here, the most interesting output of the transcriptional analysis was the role of KI in promoting the expression of the SA-related genes *PR2* and *PR5* (Fig. 6b). We also observed a strong induction of *PAD3*, which is crucial for the biosynthesis of the antimicrobial compound camalexin (Zhou et al., 1999), and, to a lesser extent, that of *ZAT12* (Fig. 6b). This is consistent with the higher H₂O₂ content quantified in the roots of 30 μ M KI-treated plants (Fig. 7a). We also noted some competition between SA and JA/ET biosynthetic genes in KI-treated plants, in favour of SA (Fig. 6a, b; Supplementary Tables S10, 11). Hormonal quantification data supported this evidence, as 30 μ M KI stimulated SA accumulation in the roots of mock-treated plants, reducing that of JA (Fig. 5b).

To the best of our knowledge, no previous studies have explicitly aimed to evaluate the effect of iodine on SA metabolism. Nevertheless, the association between iodine and SA emerged indirectly in the literature. The application of micromolar amounts of iodine, supplied as KIO₃ and/or KI, has been shown to increase SA accumulation in tomato fruits and roots (Halka et al., 2019) and in the root secretions of lettuce (Smoleń et al., 2021). In addition, gene expression profiles based on

microarray or next-generation sequencing (RNA-seq) technologies revealed the presence of a cluster of genes commonly regulated by KI/KIO₃ and SA treatments in the roots of several plant species (i.e., *Arabidopsis* - Kiferle et al., 2021; lettuce - Smoleń et al., 2023). The experiment on *Arabidopsis* mutants was used as a tool to reveal the preferential role of SA, JA and ET in the iodine-driven resistance against *B. cinerea* infection. In our selection, *sid2-3* plants are defective in the SA INDUCTION-DEFICIENT2 (SID2) gene (also named isochorismate synthase 1 (ICS1) (Pluhařová et al., 2019). The encoded enzyme converts chorismate to isochorismate, representing a crucial step in the SA biosynthesis (Rekhter et al. 2019). The *jar1-1* mutant is impaired in the JASMONATE RESISTANT 1 (JAR1) gene, which encodes a JA-amino synthetase that activates JA by conjugating it to isoleucine (Ile), having a central role in JA signalling (Staswick et al., 1992). *acs2-1acs6-1* is double knock-out mutant of two members of the multigene family encoding for 1-aminocyclopropane-1-carboxylate synthase (ACS) (Tsuchisaka et al., 2009), which converts S-adenosyl-L-methionine (SAM) to 1-aminocyclopropane-1-carboxylic acid (ACC), the immediate precursor of ethylene (Bleecker and Kende, 2000).

As a consequence, the mutation of *SID2*, *JAR1* and two members of the ACS multigene family, in our selected mutant lines leads to drastic decreases in the SA, Ja-Ile and ET levels, respectively, as widely reported in literature (e.g. *sid2-3*: Abreu et al., 2009; Pluhařová et al., 2019; *jar1-1*: Suza and Staswick, 2008; *acs2-1acs6-1*: Schellingen et al., 2014).

The analysis of the tolerance degree of the selected mutants provided a clear indication on the contribution of each hormone to the defense mechanism driven by iodine. Our results highlight that there is no preferential role of SA in tolerance to *B. cinerea* driven by iodine. Compared with that in wild-type plants, the impaired SA biosynthesis in *sid2-3* plants (Pluhařová et al., 2019) increased their resistance to the pathogen, irrespectively of KI treatment, suggesting a negative role of SA in the tolerance mechanism (Fig. 8c).

In the context of the well-characterized antagonism between SA and JA (Aerts et al., 2021; Kunkel and Brooks, 2002), the increased tolerance of *sid2-3* plants can be attributed to an increase in the JA pathway, which is crucial for plant tolerance to necrotrophic fungi, such as *B. cinerea* (Vlot et al., 2021; Li et Cheng, 2023). On the other hand, the impairment of JA signalling in *jar1-1* plants (Staswick et al., 1992), which were severely affected by the fungus, negates the positive effect of KI on their resistance (Fig. 8c), suggesting the preferential involvement of JA in the tolerance induced by iodine. Ethylene was not crucial for iodine-driven tolerance, as KI promoted the resistance of *acs2-1acs6-1* plants (Fig. 8c), which are defective in ET synthesis (Tsuchisaka et al., 2009).

5. Conclusion

Iodine has recently been demonstrated to be involved in plant nutrition, increasing plant fitness when it is applied at low concentrations and enhancing plant resistance when it is exposed to several abiotic stresses.

Our findings demonstrated a role of iodine in plant protection, as the addition of low amounts of KI (in the micromolar range) to the nutrient solution triggered, systemically, a wide range of defence-like responses. The main outcomes were the stimulatory effect of iodine on SA, JA and ET production, which are the three principal hormonal players in the pathogenic response, and the massive expression of several PRs encoding genes, possibly also mediated by H₂O₂ signalling. Iodine induced a similar response in both shoot and root tissues, even though it was more pronounced in roots, as the roots were the entry point for KI due to the cultivation system used.

The combined pattern of the results of all analysed parameters, which contrasted between iodine-supplemented and iodine-deficient plants, suggests that plant defence responses were pre-activated several days before the introduction of the pathogen. In the presence

of *B. cinerea*, the pre-activation of the defence machinery, which is mostly JA dependent, did not prevent fungal infection but strongly limited its spread.

The protective effects of iodine against *B. cinerea* infection could be stronger in the absence of the induction of SA biosynthesis triggered by iodine itself. However, the iodine-driven SA induction might represent a valuable resource to induce tolerance not only to necrotrophic fungi but also to biotrophic pathogens. Therefore, we believe that iodine is as an eco-friendly and safe priming agent having a great potential in agriculture to control a broad spectrum of plant diseases, newly underlining the benefits related to a proper integration of the element in plant nutritional programs.

Funding sources

This research was supported by Sant'Anna School of Advanced Studies (Pisa, Italy) and University of Pisa (Italy) and did not receive any specific grant from funding agencies in the public, commercial, or non-profit sectors.

CRediT authorship contribution statement

Sara Beltrami: Writing – original draft, Investigation, Data curation, Conceptualization. **Lorenzo Di Paco:** Investigation, Data curation. **Claudia Pisuttu:** Investigation, Data curation. **Lorenzo Mariotti:** Investigation, Data curation. **Alessandra Marchica:** Investigation, Data curation. **Elisa Pellegrini:** Writing – review & editing, Supervision. **Sabrina Sarrocco:** Writing – review & editing, Investigation. **Cristina Nali:** Writing – review & editing, Supervision, Funding acquisition, Conceptualization. **Pierdomenico Perata:** Writing – review & editing, Supervision, Funding acquisition, Conceptualization. **Claudia Kiferle:** Writing – review & editing, Writing – original draft, Supervision, Visualization, Project administration, Data curation, Conceptualization.

Declaration of competing interest

The authors declare that they have no known competing financial interests or personal relationships that could have appeared to influence the work reported in this paper.

Supplementary materials

Supplementary material associated with this article can be found, in the online version, at doi:10.1016/j.stress.2024.100723.

Data availability

Data will be made available on request.

References

- Abreu, M.E., Munné-Bosch, S., 2009. Salicylic acid deficiency in *NahG* transgenic lines and *sid2* mutants increases seed yield in the annual plant *Arabidopsis thaliana*. *J. Exp. Bot.* 60 (4), 1261–1271. <https://doi.org/10.1093/jxb/ern363>.
- Aerts, N., Pereira Mendes, M., Van Wees, S.C.M., 2021. Multiple levels of crosstalk in hormone networks regulating plant defence. *Plant J.* 105, 489–504. <https://doi.org/10.1111/tj.15124>.
- Ali, S., Ganai, B.A., Kamili, A.N., Bhat, A.A., Mir, Z.A., Bhat, J.A., Tyagi, A., Islam, S.T., Mushtaq, M., Yadav, P., Rawat, S., Grover, A., 2018. Pathogenesis-related proteins and peptides as promising tools for engineering plants with multiple stress tolerance. *Microbiol. Res.* 212–213, 29–37. <https://doi.org/10.1016/j.micres.2018.04.008>.
- Bleecker, A., Kende, H., 2000. Ethylene: a gaseous SIGNAL MOLECULE IN Plants. *Annu. Rev. Cell. Develop. Biol.* 16, 1–18. <https://doi.org/10.1146/annurev.cellbio.16.1.1>.
- Bi, K., Liang, Y., Mengiste, T., Sharon, A., 2023. Killing softly: a roadmap of Botrytis cinerea pathogenicity. *Trends in Plant Sci* 28 (2), 211–222. <https://doi.org/10.1016/j.tplants.2022.08.024>.
- Brown, P.H., Zhao, F.J., Dobermann, A., 2022. What is a plant nutrient? Changing definitions to advance science and innovation in plant nutrition. *Plant Soil.* 476 (1–2), 11–23. <https://doi.org/10.1007/s11104-021-05171-w>.

- Cheung, N., Tian, L., Liu, X., Li, X., 2020. The Destructive Fungal Pathogen *Botrytis cinerea*-Insights from Genes Studied with Mutant Analysis. *Pathogens*. 9 (11), 923. <https://doi.org/10.3390/pathogens9110923>.
- Davletova, S., Schlauch, K., Coutu, J., Mittler, R., 2005. The zinc-finger protein Zat12 plays a central role in reactive oxygen and abiotic stress signaling in Arabidopsis. *Plant Physiol.* 139 (2), 847–856. <https://doi.org/10.1104/pp.105.068254>.
- Dempsey, D.A., Vlot, A.C., Wildermuth, M.C., Klessig, D.F., 2011. Salicylic Acid biosynthesis and metabolism. *Arabidopsis*. Book 9, e0156. <https://doi.org/10.1199/tab.0156>.
- Ding, L.N., Li, Y.T., Wu, Y.Z., Li, T., Geng, R., Cao, J., Zhang, W., Tan, X.L., 2022. Plant disease resistance-related signaling pathways: recent progress and future prospects. *Int. J. Mol. Sci.* 23, 16200. <https://doi.org/10.3390/ijms232416200>.
- Ding, Y., Sun, T., Ao, K., Peng, Y., Zhang, Y., Li, X., Zhang, Y., 2018. Opposite roles of salicylic acid receptors NPR1 and NPR3/NPR4 in transcriptional regulation of plant immunity. *Cell* 173 (6), 1454–1467. <https://doi.org/10.1016/j.cell.2018.03.044>.
- Dos Santos, C., Franco, O.L., 2023. Pathogenesis-related proteins (PRs) with enzyme activity activating plant defence responses. *Plants* 12, 2226. <https://doi.org/10.3390/plants12112226>.
- Halka, M., Smoleń, S., Czernicka, M., Klimek-Chodacka, M., Pitala, J., Tutaj, K., 2019. Iodine biofortification through expression of HMT, SAMT and S3H genes in *Solanum lycopersicum* L. *Plant Physiol. Biochem.* 144, 35–48. <https://doi.org/10.1016/j.plaphy.2019.09.028>.
- Hönig, M., Roeber Venja, M., Schmülling, T., Cortleven, A., 2023. Chemical priming of plant defence responses to pathogen attacks. *Front. Plant Sci.* 14. <https://doi.org/10.1016/j.fpls.2022.102288>.
- Hossain, M.A., Bhattacharjee, S., Armin, S.M., Qian, P., Xin, W., Li, H.Y., Burritt, D.J., Fujita, M., Tran, L.S., 2015. Hydrogen peroxide priming modulates abiotic oxidative stress tolerance: insights from ROS detoxification and scavenging. *Front. Plant Sci.* 6, 420. <https://doi.org/10.3389/fpls.2015.00420>.
- Huang, Z.H., Wang, Z.L., Shi, B.L., Wei, D., Chen, J.X., Wang, S.L., Gao, B.J., 2015. Simultaneous Determination of Salicylic Acid, Jasmonic Acid, Methyl Salicylate, and Methyl Jasmonate from *Ulmus pumila* Leaves by GC-MS. *Int. J. Anal. Chem.* 2015, 698630. <https://doi.org/10.1155/2015/698630>.
- Huffaker, A., Pearce, G., Ryan, C.A., 2006. An endogenous peptide signal in Arabidopsis activates components of the innate immune response. *PNAS* 103 (26), 10098–10103. <https://doi.org/10.1073/pnas.0603727103>.
- Jung, H.W., Cecchini, N.M., 2023. Editorial: systemic resistance and defence priming against pathogens. *Front. Plant Sci.* 14. <https://doi.org/10.3389/fpls.2023.1267513>. <https://www.frontiersin.org/articles/10.3389/fpls.2023.1267513>.
- Kiferle, C., Martinelli, M., Salzano, A.M., Gonzali, S., Beltrami, S., Salvadori, P.A., Hora, K., Holwerda, H.T., Scalon, A., Perata, P., 2021. Evidences for a Nutritional Role of Iodine in Plants. *Front. Plant Sci.* <https://doi.org/10.3389/fpls.2021.616868>.
- Kunkel, B.N., Brooks, D.M., 2002. Cross talk between signaling pathways in pathogen defence. *Curr. Opin. Plant Biol.* 5, 325–331. [https://doi.org/10.1016/S1369-5266\(02\)00275-3](https://doi.org/10.1016/S1369-5266(02)00275-3).
- Lefevre, H., Bauters, L., Gheysen, G., 2020. Salicylic Acid Biosynthesis in Plants. *Front. Plant Sci.* 11. <https://doi.org/10.3389/fpls.2020.00338>. <https://www.frontiersin.org/articles/10.3389/fpls.2020.00338>.
- Li, R., Cheng, Y., 2023. Recent advances in mechanisms underlying defence responses of horticultural crops to *Botrytis cinerea*. *Horticulturae* 9, 1178. <https://doi.org/10.3390/horticulturae9111178>.
- Loreti, E., Valeri, M.C., Novi, G., Perata, P., 2018. Gene regulation and survival under hypoxia requires starch availability and metabolism. *Plant Physiol.* 176 (2), 1286–1298. <https://doi.org/10.1104/pp.17.01002>.
- Oberkofler, V., Pratz, L., Bäurle, I., 2021. Epigenetic regulation of abiotic stress memory: maintaining the good things while they last. *Curr. Opin. Plant Biol.*, 102007 <https://doi.org/10.1016/j.pbi.2021.102007>.
- Park, H.J., Kim, W.Y., Yun, D.J., 2016. A new insight of salt stress signaling. *Plant. Mol. Cells* 39 (6), 447–459. <https://doi.org/10.14348/molcells.2016.0083>.
- Pattyn, J., Vaughan-Hirsch, J., Van de Poel, B., 2021. The regulation of ethylene biosynthesis: a complex multilevel control circuitry. *New Phytol.* 229, 770–782. <https://doi.org/10.1111/nph.16873>.
- Pellegrini, E., Trivellini, A., Campanella, A., Francini, A., Lorenzini, G., Nali, C., Vernieri, P., 2013. Signaling molecules and cell death in *Melissa officinalis* plants exposed to ozone. *Plant Cell Rep.* <https://doi.org/10.1007/s00299-013-1508-0>.
- Perata, P., Matsukura, C., Vernieri, P., Yamaguchi, J., 1997. Sugar repression of a gibberellin-dependent signaling pathway in barley embryos. *Plant Cell* 9, 2197–2208. <https://doi.org/10.1105/tpc.9.12.2197>.
- Pluhařová, K., Leontovycová, H., Stoudková, V., Pospíchalová, R., Maršík, P., Klouček, P., Starodubtseva, A., Iakovenko, O., Krčková, Z., Valentová, O., Burketová, L., Janda, M., Kalachova, T., 2019. Salicylic Acid Mutant Collection" as a Tool to Explore the Role of Salicylic Acid in Regulation of Plant Growth under a Changing Environment. *Int. J. Mol. Sci.* 20 (24), 6365. <https://doi.org/10.3390/ijms20246365>.
- Riyazuddin, R., Singh, K., Iqbal, N., Nisha, N., Rani, A., Kumar, M., Khatri, N., Siddiqi, M. H., Yasheshwar, Kim ST, Attila, F., Gupta, R., 2023. Iodine: an emerging biostimulant of growth and stress responses in plants. *Plant Soil.* 486, 119–133. <https://doi.org/10.1007/s11104-022-05750-5>.
- Rekhter, D., Lüdke, D., Ding, Y., Feussner, K., Zienkiewicz, K., Lipka, V., Wiermer, M., Zhang, Y., Feussner, I., 2019. Isochorismate-derived biosynthesis of the plant stress hormone salicylic acid. *Science* (1979) 365, 498–502. <https://doi.org/10.1126/science.aaw1720>.
- Rizhsky, L., Davletova, S., Liang, H., Mittler, R., 2004. The Zinc Finger Protein Zat12 Is Required for Cytosolic Ascorbate Peroxidase 1 Expression during Oxidative Stress in Arabidopsis. *J. Biol. Chem.* 279, 11736–11743. <https://doi.org/10.1074/jbc.M313350200>.
- Saxena, I., Srikanth, S., Chen, Z., 2016. Cross Talk between H₂O₂ and Interacting Signal Molecules under Plant Stress Response. *Front. Plant Sci.* 7. <https://doi.org/10.3389/fpls.2016.00570>.
- Schellingen, K., Van Der Straeten, D., Vandenbussche, F., Prinsen, E., Remans, T., Vangronsveld, J., Cuypers, A., 2014. Cadmium-induced ethylene production and responses in *Arabidopsis thaliana* rely on ACS2 and ACS6 gene expression. *BMC. Plant Biol.* 14, 214. <https://doi.org/10.1186/s12870-014-0214-6>.
- Smirnoff, N., Arnaud, D., 2019. Hydrogen peroxide metabolism and functions in plants. *New Phytol.* 221, 1197–1214. <https://doi.org/10.1111/nph.15488>.
- Smoleń, S., Czernicka, M., Kowalska, I., Kęska, K., Halka, M., Grzebelus, D., Grzanka, M., Skoczylas, L., Pitala, J., Koronowicz, A., Kováčik, P., 2021. New Aspects of Uptake and Metabolism of Non-organic and Organic Iodine Compounds—The Role of Vanadium and Plant-Derived Thyroid Hormone Analogs in Lettuce. *Front. Plant Sci.* 12. <https://doi.org/10.3389/fpls.2021.653168>.
- Smoleń, S., Czernicka, M., Kęska-Izworska, K., Kowalska, I., Grzebelus, D., Pitala, J., Halka, M., Skoczylas, L., Tabaszewska, M., Liszka-Skoczylas, M., Grzanka, M., Ledwoży-Smoleń, I., Koronowicz, A., Krzemińska, J., Sularz, O., Kielbasa, D., Neupauer, J., Kováčik, P., 2023. Transcriptomic and metabolic studies on the role of inorganic and organic iodine compounds in lettuce plants. *Sci. Rep.* 13, 8440. <https://doi.org/10.1038/s41598-023-34873-7>.
- Staswick, P.E., Su, W., Howell, S.H., 1992. Methyl jasmonate inhibition of root growth and induction of a leaf protein are decreased in an *Arabidopsis thaliana* mutant. *PNAS* 89 (15), 6837–6840. <https://doi.org/10.1073/pnas.89.15.6837>.
- Suza, W.P., Staswick, P.E., 2008. The role of JAR1 in Jasmonoyl-L-isoleucine production during Arabidopsis wound response. *Planta* 227, 1221–1232. <https://doi.org/10.1007/s00425-008-0694-4>.
- Tripathi, R., Tewari, R., Singh, K.P., Keswani, C., Minkina, T., Srivastava, A.K., De Corato, U., Sansinenea, E., 2022. Plant mineral nutrition and disease resistance: a significant linkage for sustainable crop protection. *Front. Plant Sci.* 13, 883970. <https://doi.org/10.3389/fpls.2022.883970>.
- Tsuchisaka, A., Yu, G., Jin, H., Alonso, J.M., Ecker, J.R., Zhang, X., Gao, S., Theologis, A., 2009. A combinatorial interplay among the 1-aminocyclopropane-1-carboxylate isoforms regulates ethylene biosynthesis in *Arabidopsis thaliana*. *Genetics* 183 (3), 979–1003. <https://doi.org/10.1534/genetics.109.107102>.
- Valeri, M.C., Novi, G., Weits, D.A., Mensuali, A., Perata, P., Loreti, E., 2021. *Botrytis cinerea* induces local hypoxia in Arabidopsis leaves. *New Phytol.* 229, 173–185. <https://doi.org/10.1111/nph.16513>.
- Vlot, A.C., Sales, J.H., Lenk, M., Bauer, K., Brambilla, A., Sommer, A., Chen, Y., Wenig, M., Nayem, S., 2021. Systemic propagation of immunity in plants. *New Phytol.* 229, 1234–1250. <https://doi.org/10.1111/nph.16953>.
- Wasternack, C., Hause, B., 2013. Jasmonates: biosynthesis, perception, signal transduction and action in plant stress response, growth and development. An update to the 2007 review in *Annals of Botany*. *Ann. Bot.* 111 (6), 1021–1058. <https://doi.org/10.1093/aob/mct067>.
- Zhang, Y., Cao, H., Wang, M., Zou, Z., Zhou, P., Wang, X., Jin, J., 2023. A review of iodine in plants with biofortification: uptake, accumulation, transportation, function, and toxicity. *Sci. Total Env.* 878, 163203. <https://doi.org/10.1016/j.scitotenv.2023.163203>.
- Zhou, M., Wang, W., 2018. Recent Advances in Synthetic Chemical Inducers of Plant Immunity. *Front. Plant Sci.* 9, 1613. <https://doi.org/10.3389/fpls.2018.01613>.
- Zhou, N., Tootle, T.L., Glazebrook, J., 1999. Arabidopsis PAD3, a gene required for camalexin biosynthesis, encodes a putative cytochrome P450 monooxygenase. *Plant Cell* 11 (12), 2419–2428. <https://doi.org/10.1105/tpc.11.12.2419>.
- Zubrod, J.P., Bundschuh, M., Arts, G., Brühl, C.A., Imfeld, G., Knäbel, A., Payraudeau, S., Rasmussen, J.J., Rohr, J., Scharmüller, A., Smalling, K., Stehle, S., Schulz, R., Schäfer, R.B., 2019. Fungicides: an Overlooked Pesticide Class? *Environ. Sci. Tech.* 53 (7), 3347–3365. <https://doi.org/10.1021/acs.est.8b04392>.